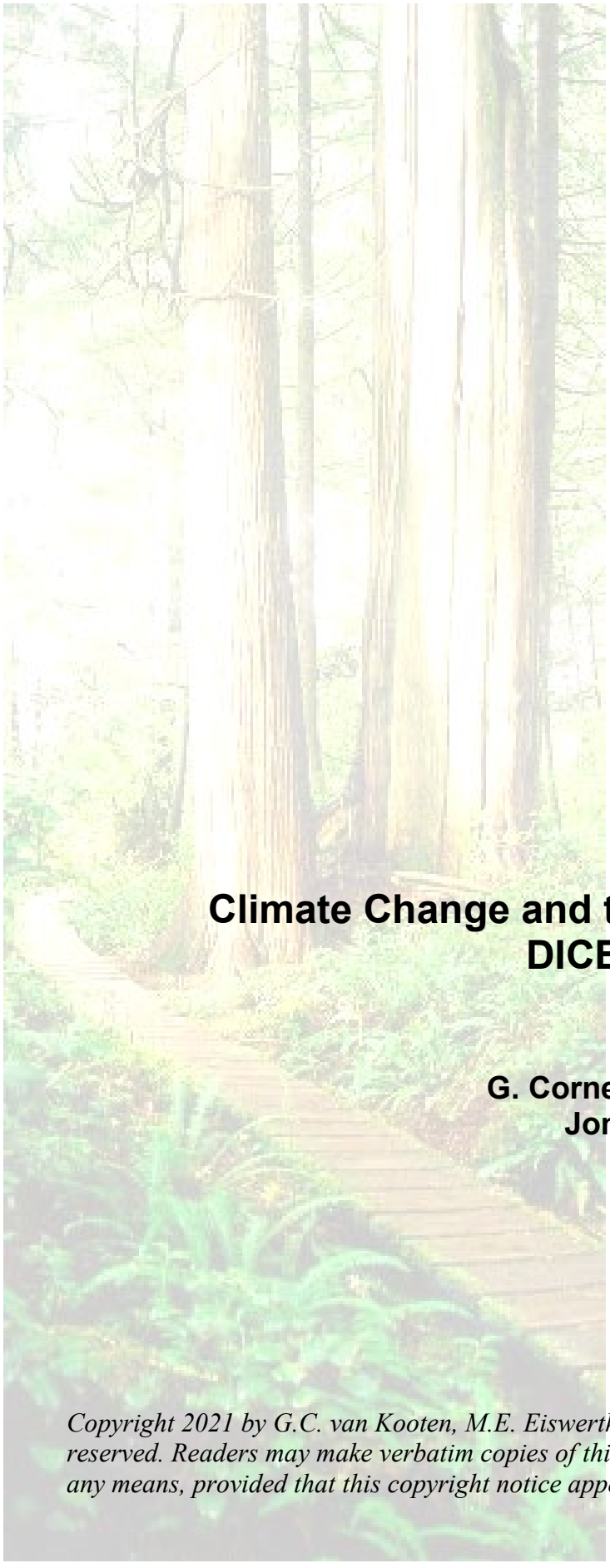

WORKING PAPER
2021-01

REPA

Resource Economics
& Policy Analysis
Research Group

Department of Economics
University of Victoria

Climate Change and the Social Cost of Carbon: DICE Explained and Expanded

G. Cornelis van Kooten, Mark E. Eiswerth,
Jonathan Izett and Alyssa R. Russell

June 2021

For copies of this or other REPA working papers contact:

REPA Research Group
Department of Economics
University of Victoria PO Box 1700 STN CSC Victoria, BC V8W 2Y2 CANADA
repa@uvic.ca

http://web.uvic.ca/~repa/

CLIMATE CHANGE AND THE SOCIAL COST OF CARBON: DICE EXPLAINED AND EXPANDED

G. Cornelis van Kooten, Mark E. Eiswerth, Jonathan Izett and Alyssa R. Russell[1]

DRAFT: June 2, 2021

Abstract

In this background paper, we describe the science that underlies climate models. We then develop several energy balance models (EBMs), including the carbon-climate module found in Nordhaus' Dynamic Integrated Climate Economic (DICE) model. The climate model in DICE is modified to track the average path of temperatures from the CMIP5 ensemble. The parameterization of the DICE model is described. Finally, the re-parameterized DICE model is then modified to investigate the impact that a global effort to increase forest growth would have on the social cost of carbon.

Key Words: climate science and climate modelling; energy balance; ocean heat; climate feedbacks; reforestation

JEL Categories: Q54, C61, E17, F64, H23,

[1] The authors wish to acknowledge financial support from Canada's SSHRC Insight Grant Program (PDG 890-2016-0064). They declare no competing interests.

1. INTRODUCTION

Climate change is one of the most contentious policy issues of the early 21st Century. In December 2015, nations signed the Paris Agreement, which aims "to strengthen the global response to the threat of climate change by keeping a global temperature rise this century well below 2 degrees Celsius (°C) above pre-industrial levels and to pursue efforts to limit the temperature increase even further to 1.5°C. Additionally, the agreement aims to strengthen the ability of countries to deal with the impacts of climate change" (United Nations, 2015). Subsequently, the U.S. Fourth National Climate Assessment (NCA) expressed fear that "climate change creates new risks and exacerbates existing vulnerabilities in communities across the United States, presenting growing challenges to human health and safety, quality of life, and the rate of economic growth" (Reidmiller et al., 2017). Climate change and how to prevent it from happening has become the 21st Century's most contentious policy issue. However, to determine whether mitigation is worthwhile undertaking it is necessary to know something about the marginal damage (MD) from emitting another tonne of CO_2 (tCO_2). The MD is needed to guide the development of climate change mitigation policies.

Climate change is a contentious policy issue (Tol 2014; Nordhaus 2013). There is a great deal of uncertainty concerning climate change, especially regarding (1) the projected increase in average global temperatures (McKitrick & Christy 2019a; Lewis & Curry 2018; Hourdin et al. 2017; Millar et al. 2017; McKitrick & Vogelsang 2014); (2) the regional changes in climate that might be expected (Koonin 2021; McKitrick & Christy 2019b; Pielke 2018; Lomborg 2007); and (3) the contribution to global warming of human activities (e.g., burning of fossil fuels, land use changes) versus that of natural factors (e.g., CO_2 release from or absorption by oceans, changes in the sun's activities) (Koutsoyiannis 2021; Maher et al. 2020; Lindzen 2020; Zharkova et al. 2019;

Frank 2019; Richard 2019; de Larminat 2016, 2019; Svensmark et al. 2017; McKitrick & Nierenberg 2011; McKitrick & Michaels 2004, 2007; Khilyuk & Chilingar 2006; de Laat & Maurellis 2004, 2006). With respect to the latter, it is worth noting that Article 1 of the United Nations Framework Convention on Climate Change (UNFCCC) of 1992 defines 'climate change' as: *"a change of climate which is attributed directly or indirectly to human activity that alters the composition of the global atmosphere and which is in addition to natural climate variability observed over comparable time periods*."

There is also controversy concerning the way in which the mean surface temperatures are estimated, especially how weather-station data are averaged over a certain area (Essex and McKitrick 2002; van Kooten 2013, pp.16-48). Some have argued that past surface (and ocean) temperatures have been lowered, thereby making more recent temperatures appear higher (Hoven 2012; see also IPCC 2013, pp.188-189).[2] Whether this is the case is likely to remain controversial, but it is now well established that temperatures during the Medieval Warm Period (circ 12th Century) may have been warmer than currently—that the so-called 'hockey stick' graph of temperatures has been refuted (see McIntyre & McKitrick, 2009; van Kooten 2013, pp.71-97; McKitrick 2015). Further, there are questions regarding the appropriateness of using the Earth's mean surface temperature as the indicator of climate change. Given that climate models focus on changes in the atmosphere, it is atmospheric temperatures that are important, especially the temperature in the troposphere (or about 10 km) above the tropics where the first evidence of warming is supposed to occur (e.g., see Christy & McNider 2017; IPCC 2001, pp.695-738).

[2] See also Investor's Business Daily editorial (29-Mar-2018), 'The Stunning Statistical Fraud Behind The Global Warming Scare' at https://www.investors.com/politics/editorials/the-stunning-statistical-fraud-behind-the-global-warming-scare/ [accessed May 7, 2021]. See Dahlman & Lindsey (2020) for a description regarding measurement of ocean temperatures using Argo buoys.

The current study focuses on economic aspects of global warming, primarily the need to examine costs and benefits. The types of models that economists employ begin by assuming that CO_2 emissions from fossil fuel use lead to rising concentrations of atmospheric CO_2 that, in turn, results in damages to the economy. As noted, considerable uncertainty exists regarding the potential damages from future climate change, which, in turn, constitute the benefits of mitigating (avoiding) global warming. This is seen in the controversy concerning estimates of marginal damages, which depend crucially on estimates of expected damages (e.g., Auffhammer 2018; Dayaratna et al. 2017; Pindyck 2013). For instance, many damage estimates concern goods and services that are not traded in markets (e.g., wetland services, biodiversity, heat and mental stress, threats to national security), and thereby are not easily valued. It is difficult to determine how climate change affects these types of things, let alone place a value on the changes that occur.[3]

Policymakers need estimates of marginal damages—also referred to as the social cost of carbon (SCC)—to guide decisions about carbon taxes and for determining the benefits (damages avoided) of mitigation strategies. SCC estimates are available from three integrated assessment models (IAMs), two of which are open source—William Nordhaus' Dynamic Integrated Climate and Economics (DICE) model (Nordhaus 2013, 2018a, 2019) and Richard Tol's Climate Framework for Uncertainty, Negotiation and Distribution (FUND) model (Tol 2014).[4] Such IAMs have been criticized by both economists and climate scientists. For example, Robert Pindyck (2013, 2017) finds that models are too ad hoc, with outcomes highly sensitive to assumed parameter values. Nicholas Lewis (2018) finds that the parameterization of the carbon-climate

[3] Many argue that climate change is already happening, citing increases in droughts, wildfire, floods, hurricanes and other weather events as evidence. Such evidence simply does not exist. Even the IPCC concludes that there is still no evidence that harmful weather events have increased as the globe has warmed since pre-industrial times. See Alexander (2020, 2021) and Goklany (2021) and references therein.
[4] The third is the Policy Analysis of the Greenhouse Effect (PAGE), which is not open source (Hope 2006).

component of the DICE model, in particular, is faulty. Not surprisingly, the same is true of the climate models themselves (Lewis & Curry 2015, 2018; Hourdin et al. 2017; Millar et al. 2017; Voosen 2016). Despite such criticism, IAMs offer one of the only ways that economists can provide policy advice that is informed by the findings of the climate models and the Shared Socioeconomic Pathways (SSPs), or storylines, that are used to determine the Representative Concentration Pathways (RCPs) of future CO_2 emissions (Riahi et al. 2017; van Vuuren et al. 2011).

In this paper, we employ the DICE model to investigate two particular aspects related to the estimation of marginal damages, or SCC. First, the objective in DICE is to maximize the present value of the per capita utility that people get from consumption, subject to various economic, biophysical and climate constraints. Since utility from consumption accrues over a period of 100 or more years, the issue is intergenerational and sensitive to the choice of discount rate. Further, DICE outputs depend on assumptions regarding the causal relationship between CO_2 emissions and temperature, and then between temperature and economic damages, relationships that are derived from global climate models. The carbon, temperature and damage components in DICE are sensitive to the parameterizations employed. We use Monte Carlo simulation over a variety of model components to examine the sensitivity of SCC to various parameterizations.

Second, the SCC changes over time partly because, when another tCO_2 is released to the atmosphere, it creates a higher level of damage than the previous tCO_2—damages rise at an increasing rate. But there is more to it than this, because the timing of CO_2 should work in the opposite direction—future emissions of CO_2 should be worth less than today's emissions, particularly if there is some urgency to mitigate global warming. Clearly, any CO_2 removed from the atmosphere in 20 or more years from now, say by growing trees, is irrelevant if there is a

climate emergency. However, future carbon fluxes are not treated as if they are worth less than current fluxes, because the intergenerational discount rate is too low. That is, the rate used to discount the future (the social rate of time preference plus the elasticity of marginal utility of per capita consumption multiplied by the rate of change in consumption) is some 3% to 4% (it actually changes over time and is sensitive to the elasticity of the marginal utility of consumption). If the marginal damage (SCC) rises at an annual rate of 3.6%, the effective rate at which future carbon fluxes are discounted could be positive (4.0% minus 3.6%) or even negative (3.0% minus 3.6%). Future carbon fluxes might be inflated relative to today or they are discounted at a near zero rate. These low or negative rates provide an incentive to move forward emissions of CO_2 (whenever possible) but delay removals of CO_2 from the atmosphere (e.g., growing trees), perhaps indefinitely if the effective rate is negative. Yet, if there is some urgency in addressing climate change, the rate used to discount future CO_2 emissions should be much higher (van Kooten et al. 2021; van Kooten & Johnston 2016; Johnston & van Kooten 2015). Urgency is a policy variable but it gets entangled with the intergenerational discount rate used for monetary values (van Kooten 2021, pp.41-46). These rates are different and we demonstrate why and, using the DICE model, the implications this could have for mitigation activities.

The paper is structured as follows. Since we considerably modify Nordhaus' (2018b, 2017) DICE model (version 2016R2-083017), we need to discuss the various changes that we made to the key model equations. One of these relates to the modeling of the carbon component of the model; we explain the parameters that Nordhaus used so that our assumptions are clarified. The DICE model can be decomposed into three major components: (1) the objective function; (2) the carbon and climate modules; and (3) the economic component, which includes emissions and damages. Rather than beginning with the objective function, we first consider the carbon and

climate modules. We do this by starting in Section 2 with a discussion of climate models more generally. In Section 3, we develop different climate models that can be used in the DICE model. In Sections 4 and 5, we discuss the basics of the DICE model's objective function component as well as an application of the DICE model to investigate the economics of forestlands restoration for climate change mitigation. Finally, we offer a concluding discussion including the next steps we plan to undertake for future research.

2. CARBON AND CLIMATE COMPONENTS OF THE DICE MODEL

Background Physics

Averaged over the entire surface of the Earth, net incoming energy represents about 342 Watts per square meter (W/m^2) of incident solar irradiance. Of the 342 W/m^2, about 240 W/m^2 makes it into the Earth's atmosphere, with the difference scattered by air, water vapor and aerosols, or reflected by clouds or even by the Earth's surface. About 65 W/m^2 is absorbed by the atmosphere and clouds, while 175 W/m^2 actually reaches the Earth's surface where it is absorbed. Outgoing longwave radiation emitted from the atmosphere into space represents an energy loss to space of some 235 W/m^2 (or 40.7% of total incoming solar energy). These numbers are approximations as they depend on a large number of factors, including the location of the Earth relative to the sun, solar activity, the Earth's albedo, the heat absorbed by so-called greenhouse gases (GHGs), cloud cover, et cetera. The difference between the incoming (mainly shortwave) radiation and the outgoing (longwave) radiation is referred to as the *radiative forcing*, and it makes the Earth's temperature warm enough for life.

How do we measure the warming effects of incoming versus outgoing radiation—the radiative forcing and the impact of humans on the system? Consider first the Stefan-Boltzmann law that gives the irradiance (F) or outgoing radiation from any blackbody (Wallace and Hobbs

2006, p.117; Pierrehumbert 2011; Happer 2019):

$$F(T) = -\sigma T^4 \ [\mathrm{W} \cdot \mathrm{m}^{-2}], \quad (1)$$

where $\sigma = 5.67 \times 10^{-8}$ W · m^{-2} · K^{-4} is the Stefan-Boltzmann constant and T refers to temperature. Unlike a pure blackbody, the Earth is characterized by clouds that reflect light and an atmosphere that reflects and scatters light and absorbs some of the outgoing radiation. Calculating the radiative forcing is not straightforward, because there are different ways to calculate the amount of solar energy that gets absorbed by the Earth's surface and atmosphere.

By modifying the Stefan-Boltzmann law, it is possible to determine the solar energy flux or irradiance (also known as insolation) reaching the Earth, symbolized by S_0 and measured in W/m^2 [W · m^{-2}]. The solar energy flux varies with the distance from the sun according to:

$$S_0 = \sigma T_{sun}^4 \frac{r_{sun}^2}{d_{ES}^2}, \quad (2)$$

where d_{ES} is the distance between the Earth and the sun. Given that the average surface (but not core) temperature of the sun is 5,780 degrees Kelvin (K), the radius of the sun is 695,500 km, and the average distance from the Earth to the sun is 149.6 million km, then $S_0 = 1{,}367.81$ W · m^{-2}. This is the solar constant for the Earth, although it will differ throughout the year as the distance between the sun and the Earth varies. Upon dividing by four to determine the incident solar radiation over the Earth's surface exposed to the sun at any time, we get an average radiation of 342 W · m^{-2}.

The surface area of a sphere is equal to $4\pi r^2$, where r is the radius of the sphere. Since about one-quarter of the Earth's overall surface is directly exposed to the sun at any time, the solar energy that reaches the Earth at any time is given by $S_0 \pi r^2$, where r refers to the radius of the Earth (6,378

km).[5] Earth has a surface area of approximately 5.114×10^{14} m^2. If the Earth was a perfect blackbody, it would radiate energy according to the Stefan-Boltzmann law (1), but then from the entire sphere and not just that part exposed to the sun. This implies that, as a blackbody, the Earth would radiate energy to space according to $4\,\sigma\,T^4\,\pi\,r^2$. At the same time, it would absorb energy from the sun according to $S_0\,\pi\,r^2$. Equating these two expressions gives:

$$S_0\,\pi\,r^2 = 4\,\sigma\,T^4\,\pi\,r^2 \Rightarrow S_0 = 4\,\sigma\,T^4. \quad (3)$$

Solving result (3) for T gives the average temperature of the Earth if it had no atmosphere. The result is a temperature of 278.67 K, or 5.52ºC (given that absolute zero is –273.15 K). The average surface temperature of the Earth is actually about 15ºC because the Earth is not a blackbody.[6] While the atmosphere scatters and reflects light, it also absorbs some outgoing radiation, thereby warming the Earth. The role of anthropogenic emissions of CO_2 and other GHGs, which we lump together under the rubric of CO_2, plays out in the atmosphere only.[7]

Solar irradiation (insolation) constitutes one type of forcing, while human emissions of CO_2 constitute another. The total radiative forcing historically consists of anthropogenic, volcanic and solar contributions (de Larminat 2019):

$$F = F_{anth} + F_{volc} + F_{sol}. \quad (4)$$

This can be rewritten to reflect the relationship between real radiative forcing, denoted F_x, and the a priori forcing, f_x, with $F_x = a_x \times f_x$, where a_x are scaling factors associated with forcing type x and

[5] We divide the area of a sphere, given by $4\,\pi\,r^2$, by 4 to account for the fact that only one-quarter of the Earth's surface is exposed to the sun at any given time.

[6] The average temperature of the Earth in 2017 was 14.9ºC https://www.space.com/17816-earth-temperature.html [accessed May 4, 2021].

[7] Under idealized dry conditions, nitrogen constitutes about 78% of the atmosphere, or 780,840 parts per million by volume (hereafter ppm); oxygen (O_2), 20.9% (209,460 ppm); argon (Ar), 0.93% (9,340 ppm); carbon dioxide (CO_2), 0.041% (410 ppm), varying by season and increasing; methane (CH_4), 0.00018% (1.79 ppm); nitrous oxide (N_2O), 0.0000325% (0.325 ppm); and ozone (O_3), 0 to 0.000007% (0.0-0.07 ppm). CO_2, CH_4, N_2O and O_3 constitute the greenhouse gases, along with water vapor (H_2O).

these should be close to 1.0. Then, following de Larminat (2019), we rewrite (4) as:

$$F = a_{anth} f_{anth} + a_{volc} f_{volc} + a_{Lsol} f_{Lsol} + a_{Hsol} f_{Hsol}, \quad (5)$$

where the single solar signal is divided into a low- and a high-frequency component. De Larminat (2019) estimated the scaling factors using observational data, and these values are discussed further in the context of climate models. We will not consider further the volcanic forcing except to provide some notion of its contribution.

Anthropogenic Forcing

The anthropogenic forcing is the result of CO_2 (including other GHG) emissions and removals, and works as follows. Because longwave infrared radiation (IR) emanates from the surface of the Earth, some of the CO_2 molecules, which constitute about 0.04% of the volume of the atmosphere, enter into a higher vibrational mode by absorbing IR in the 14-16-micrometer (μm) range. This does not, in and of itself, raise the temperature of the atmosphere. The CO_2 molecules might simply re-radiate the energy into the atmosphere and no warming occurs. More likely, the excited CO_2 molecules will collide with other molecules, such as N_2, O_2 and H_2O, thereby transferring their vibrational energy into thermal energy (speeding up the other molecules), leading to a rise in atmospheric temperature. This constitutes a positive feedback to the initial CO_2 forcing.[8]

As indicated in Table 1, during the industrial era the radiative forcing due to well-mixed GHGs is estimated to be 2.83 W/m^2, with a range of 2.54 to 3.12 W/m^2; CO_2 contributed nearly 65% of the GHG forcing since 1750, or 1.84 W/m^2. The radiative forcing of CO_2 is determined to increase as the concentration of CO_2 in the atmosphere increases and is currently assessed to be

[8] The absorption of thermal radiation by GHG molecules occurs mainly as a result of oscillating electric dipole moments induced by vibrations and rotations of these molecules. Since N_2 and O_2 produce no oscillating dipole movement, they absorb no thermal radiation. One effect of the slight warming caused by CO_2 is an increase in humidity due to the atmosphere's ability to hold more H_2O, which, because molecules of H_2O produce oscillating dipole movements, absorb additional radiant heat.

increasing at a rate of 0.3 W/m^2 per decade (IPCC 2013, p.676).

Table 1: Global Mean Radiative Forcing, 1750 to 2011[a]

Source	RF (W/m^2)[a]	Range (W/m^2)
Total anthropogenic forcing	+2.30	[+1.10, +3.30]
Well-mixed GHGs (CO2, CH4, N2O, CFC, halocarbon)	+2.83	[+2.54, +3.12]
Aerosol-radiation interaction[b]	–0.45	[–0.95, +0.05]
Aerosol-cloud interaction	–0.45	[–1.20, +0.00]
Troposphere ozone	+0.40	[+0.20, +0.60]
Stratosphere ozone	–0.05	[–0.15, +0.05]
Stratosphere water vapor	+0.07	[+0.02, +0.12]
Surface albedo (land use)	–0.15	[–0.25, –0.05]
Surface albedo (black carbon aerosol on snow & ice)	+0.04	[+0.02, +0.09]
Combined contrails & contrail-induced cirrus	+0.05	[+0.02, +0.15]
Solar irradiance	+0.05	[+0.00, +0.10]

[a] Effective radiative forcing (ERF) is used rather than radiative forcing (RF) where they differ, because ERF has been shown to be a better indicator of the global mean surface temperature (GMST) response and is emphasized by the IPCC (2013, p.53 of Technical Summary).
[b] Biomass burning is neutral, although in previous reports it was negative and then slightly positive in AR4 (IPCC 2007).
Source: IPCC (2013, Table 8.6, p.696).

The anthropogenic radiative forcing for a doubling of CO_2 is $F_{2\times CO2} \approx 3.7\ \mathrm{W \cdot m^{-2}} \approx 5.35 \ln(2)\ \mathrm{W \cdot m^{-2}}$. The anthropogenic a priori forcing factor is then given by

$$F_{anth,t} = F_{2\times CO2} \times \frac{ln\left(\frac{CO_{2,t}}{CO_{2,I}}\right)}{ln(2)}, \tag{6}$$

where $CO_{2,I}$ refers to the pre-industrial (1750) level of atmospheric CO_2, which is usually taken to be about 280 ppm. Employing equation (6), and an atmospheric CO_2 concentration of 415 ppm, the anthropogenic forcing equals 2.10 $\mathrm{W \cdot m^{-2}}$. What will it be in 2100? The forcing in the year 2100 depends on a variety of factors, including the value of $F_{2\times CO2}$ and the rate at which the radiative forcing of CO_2 is considered to be increasing, and on how much anthropogenic CO_2 will be emitted to the atmosphere in the next eight decades.

Solar Forcing

Notice that, from Table 1, the role of the sun is considered to be minimal. Variations in solar irradiation are considered by the IPCC to be extremely small compared to CO_2 (recall we assume CO_2 includes other GHGs). This is in keeping with the view that the forcing caused by the sun has

changed little over the past millennia, as evidenced by the 'hockey stick' graph (van Kooten 2013, pp.78-95). In contrast, using observational data, some researchers have determined that solar forcings actually dominate anthropogenic ones (e.g., Khilyuk & Chilingar 2006; de Larminat 2016, 2019; Svensmark et al. 2017; Zharkova et al. 2019).[9]

Feedbacks and Mean Surface and Ocean Temperatures

Any forcing or perturbation can have exacerbating (positive) or suppressing (negative) feedbacks. For example, if there is a perturbation that causes temperatures to fall, more snow and ice are likely; snow and ice lead to an albedo reflecting sunlight back to space, thereby enhancing the original cooling. Thus, snow and ice formation constitute an exacerbating feedback because they tend to reduce further the original reduction in temperature. Conversely, the warming effect of increased atmospheric CO_2 will tend to reduce snow and ice, thereby reducing the Earth's albedo and increasing its temperature. Likewise, a warmer atmosphere will hold more water vapor, which is a potent GHG that amplifies the initial warming due to CO_2 and other trace GHGs such as methane (CH_4), nitrous oxide (N_2O) and chlorofluorocarbons (HFCs).[10] To determine the impact of human emissions of CO_2 on climate, therefore, we need to take into account related feedbacks, which can either amplify or dampen the forcing from adding CO_2 into the atmosphere.

Feedbacks are crucial for determining the anthropogenic impact on average global temperature. Suppose anthropogenic emissions of CO_2 introduce a forcing F into the system, where there was none previously and temperatures had remained constant. With the CO_2 forcing, the system will, over time, come back to a new (higher) temperature equilibrium given by the

[9] A common conclusion concerning attribution of climate change is the following: "The unavoidable conclusion is that a temperature signal from anthropogenic CO_2 emissions (if any) cannot have been, nor presently can be, evidenced in climate observables" (Frank 2019, p.14).

[10] But see Koutsoyiannis (2021), who argues that climate models are wrong because they assume climate to be a static concept rather than a stochastic one, claiming instead that water controls the climate, not CO_2.

following equation (McGuffie and Henderson-Sellers 2009, p.39; Spencer & Braswell 2010; Pretis 2020):

$$\frac{dT_m}{dt} = \frac{1}{C_m}(F - \lambda\, T_m), \qquad (7)$$

where T_m is the temperature departure from a long-term average equilibrium (ºC or K) of system component m; dt represents the time step;[11] C_m is the effective heat capacity of system component m—the energy required to change the temperature of the component by 1ºC; F is the externally prescribed net radiative forcing ($W \cdot m^{-2}$); and λ is the total feedback parameter ($W \cdot m^{-2} \cdot K^{-1}$). If T refers to the mean global average surface temperature, we can write the temperature departure from its long-run average at any time t as $T_t = T_{S,t} - T_I$, where $T_{S,t}$ is the surface temperature at time t and T_I the pre-industrial temperature. The term λT_m thus captures the increasing outgoing longwave radiation as temperatures rise.

The effective heat capacity of the atmosphere is the amount of energy required to heat up the surface by 1ºC. It equals the total mass multiplied by its specific heat at constant pressure:

$$C_A = c_p\, p_a / g = (1{,}006\ J \cdot kg^{-1} \cdot K^{-1} \times 10^5\ Pa) / (9.81\ m \cdot s^{-2}) = 1.025 \times 10^7\ J \cdot K^{-1} \cdot m^{-2}, \qquad (8)$$

where p_a is the atmospheric pressure (1 bar), c_p is the specific heat capacity of the atmosphere, and g refers to the gravitational force (Hartmann 2016). For the atmosphere, c_p equals $1.006\ kJ \cdot kg^{-1} \cdot K^{-1}$ at 1 bar of atmospheric pressure (the subscript in c_p refers to pressure).[12]

Likewise, we can find the total effective heat capacity of the ocean as its mass times the specific heat at some depth:

$$C_O = p_w\, c_w\, d = d \times 10^3\ kg \cdot m^{-3} \times 4{,}187\ J \cdot kg^{-1} \cdot K^{-1} = d \times 4.187 \times 10^6\ J \cdot K^{-1} \cdot m^{-3}, \qquad (9)$$

[11] The time step differs from e-folding time, which is the time interval in which an exponentially growing quantity increases by a factor of e=2.71828; thus, it is the base-e analog of doubling time.
[12] In terms of conversions, 1 bar = 10^5 Pa, where a Pascal (Pa) = $1\ N \cdot m^{-2} = 1\ kg \cdot m^{-1} \cdot s^{-2} = 1\ J \cdot m^{-3}$.

where p_w is the density of water (1000 kg/m^3), c_w is the specific heat capacity of water (4.187 kJ · kg^{-1} · K^{-1}), and d is the depth of the ocean (Hartmann 2016; McGuffie and Henderson-Sellers 2009, p.84). For the ocean, c_w varies from 4.000 through 4.011 kJ · kg^{-1} · K^{-1}, depending on the ocean temperature and saturation pressure.[13] If the depth of the upper ocean is taken to be 75 m (see Table 2), then its heat capacity is $C_O = 3.14025 \times 10^8$ J · K^{-1} · m^{-2}. If the upper ocean depth is 150 m, the heat content would be $C_O = 6.2805 \times 10^8$ J · K^{-1} · m^{-2}. The total heat capacity of the mixed atmosphere-ocean layer equals the sum of the heat capacities of the atmosphere and upper ocean; for a depth of 150 m, $C_{AO} = 6.3830 \times 10^8$ J · K^{-1} · m^{-2}. These values would be used in a simple one-layer, mixed atmosphere-ocean model.

One mole of CO_2 has a weight of 44.0087 grams (g),[14] composed of 12.0107 g of carbon and two times 15.999 g of oxygen. Upon multiplying the CO_2 atmospheric volume by 44.0087 g CO_2 and then dividing by 28.971 g/mole, which is the average molar mass of dry air, we get the percent of CO_2 in the atmosphere by mass rather than volume.[15] For example, if the concentration of CO_2 in the atmosphere is 415 ppm, then we have the following mass of carbon in the atmosphere as a percent:

[13] See Engineering Toolbox at https://www.engineeringtoolbox.com/sea-water-properties-d_840.html [accessed May 7, 2021]. For the ocean, at a temperature of 12°C and saturation pressure of 0.01374 bar, the heat capacity c_w equals 4.003 kJ · kg^{-1} · K^{-1}. For water, the specific heat capacity of water is simply 4.187 kJ kg^{-1} K^{-1}.

[14] Here g denotes grams, although in equation (8) and later on g is also used to denote the gravity constant. It should be clear which is which from its context.

[15] See http://www.grisanik.com/blog/how-much-carbon-is-in-the-atmosphere/ [accessed May 7, 2021]. See also Moore (2016).

Table 2: Physics of Climate Change: Parameters

Parameter	Value[a]	Units of measurement
Total mass of the atmosphere	5.148×10^{18}	kg
Water vapor mass	12.7×10^{15}	kg
Surface area of the Earth	5.114×10^{14}	m^2
Surface area of the oceans	3.580×10^{14}	m^2
Specific heat capacity of oceans	4187 [4200]	$J\ kg^{-1}\ K^{-1}$
Heat flux of global ocean surface		
1971 – 2010	0.55	$W\ m^{-2}$
1993 – 2010	0.71	$W\ m^{-2}$
Ocean warming rate		
Upper 75 m of ocean	0.11 [0.09, 0.13]	°C per decade
At 200 m	0.04	°C per decade
At 700 m	0.015	°C per decade
At 3,000 m	0.01	°C per decade
Average ocean heat gain rates 1993 – 2017		
0 to 700 m depth	0.36 – 0.40	$W\ m^{-2}$
700 to 2,000 m depth	0.19 – 0.35	$W\ m^{-2}$
Average Earth energy gain 1971 – 2010	0.42	$W\ m^{-2}$

[a] Alternative values or ranges are provided in square parentheses.
Sources: Trenberth & Guillemot (1994); Dut (1998); Trenberth & Smith (2005); McGuffie & Henderson-Sellers (2009); Levitus et al. (2012); IPCC (2013, pp. 260-266); NOAA (2018).

$$\begin{aligned} \%\ \text{Mass carbon} &= 0.0415\% \times 44.0087\ g \cdot CO_2 \cdot mole^{-1} / 28.971\ g \cdot mole^{-1} \\ &= 0.06304\%\ CO_2\ \text{by mass} \end{aligned} \quad (10)$$

Multiplying by the mass of the atmosphere given in Table 2 leads to a total carbon mass of 3,245.30 Gt CO_2. Assuming that, in 1750, the concentration of CO_2 in the atmosphere was 280 ppm, CO_2 accounted for 0.042534% of the mass of the atmosphere, or total mass of 2,189.65 Gt CO_2. In 1900, the atmospheric concentration of CO_2 was 295.7 ppm, which translates into 0.04492% of the atmosphere's mass, or 2,312.48 Gt CO_2.

The oceans store some 38,000 Gt carbon or approximately 140,000 Gt CO_2. Of this amount, we allocate 7.5% to the upper 150 m ocean layer and the remainder to the deep ocean to 2,000 m. This gives inventories of approximately 10,500 Gt CO_2 in the upper ocean and 129,000 Gt CO_2 in the deep ocean.

How large are the feedbacks associated with the anthropogenic forcing? The feedback from clouds remains the largest uncertain feedback and probably the most controversial (Knutti et al. 2017; Svenmark et al. 2017; Koonin 2021, Chapter 7). As more water vapor enters the atmosphere,

some of the vapor turns to water resulting in cloud formation. Clouds consist of water and water vapor; they have a warming effect because they control release of longwave radiation, but they also increase albedo resulting in cooling. The albedo effect is greater than the greenhouse effect for clouds that form in the low to mid atmosphere, while the opposite occurs for cirrus clouds that tend to be more pervious to solar insolation. However, "it will take decades before clouds can actually be resolved in climate change simulations using global [climate] models because of the required resolution, even if computing capacity continues to increase as it has" (Knutti et al. 2017, p. 731).[16]

Transient and Equilibrium Climate Responses

Knutti et al. (2017) define the transient climate response (TCR) as the global mean surface warming from a doubling of CO_2 in an experiment with an idealized 1% per year increase in atmospheric CO_2 as determined by climate models; that is, it is an estimate of the warming resulting from a doubling of CO_2 over a 70-year time period (as $1.01^{70} = 2.00$), without allowing for the oceans to fully adjust. The a priori radiative forcing for a doubling of CO_2 is: $F_{2\times CO2} = 3.7$ W/m^2, as discussed in the context of equation (6); it reflects the value used in recent studies (Knutti et al. 2017). Another more recent measure is the transient response to carbon emissions (TCRE), which measures the change in global mean surface temperature at the end of a period, typically 100 years, during which 1,000 GtC (or 3,667 Gt CO_2) is emitted at a steady rate.[17]

In contrast, the equilibrium climate sensitivity (ECS) is defined as the equilibrium warming

[16] As Happer (2019) points out in a section on 'Numerical Modeling', if one is to characterize a 100 km thick atmosphere, climate models would need to store more than 250 billion numbers just to describe a dry atmosphere. Yet, the latest climate models find that less clouds form in the lower atmosphere resulting in greater warming as less solar irradiance reflects back to space (Zelinka et al. 2020; also see Koonin 2021, Chapter 4).

[17] See https://judithcurry.com/2019/12/23/3-degrees-c/ or https://en.wikipedia.org/wiki/Climate_sensitivity [both accessed 02 June 2020].

that occurs as a result of doubling the concentration of CO_2 in the atmosphere, but disregarding the Earth's feedbacks. ECS represents the long-run temperature increase associated with a doubling of atmospheric CO_2 above its pre-industrial level, followed by no further CO_2 emissions, and then after allowing sufficient time for the deep ocean to return to equilibrium in response to surface warming (which could take as much as a 1000 years). Therefore, ECS must be greater than TCR. Projections of future warming are particularly sensitive to the choices of these parameters.

What are the values of ECS and TCR? Three approaches have been employed to estimate these values: (i) estimates based on actual observations; (ii) estimates obtained from climate models; and (iii) estimates based on physics. First consider observation based estimates. Using 1869-1882 as a base period and 2007-2018 as a final period (ΔT), Lewis and Curry (2018) find a median value for ECS of 1.50 K (range: 1.05-2.45 K) and a median value for TCR of 1.20 K (range: 0.90-1.70 K); however, if in-filled global temperature data are employed, estimates are somewhat higher, namely, 1.66 K (1.15-2.70 K) and 1.33 K (1.00-1.90 K) for ECS and TCR, respectively. Using co-integrated vector autoregressive models, Pretis (2020) estimates values of ECS of 1.37-1.67 K in his main model, but finds a value of 2.16 K in his 'preferred model'. He estimates TCR values of 1.24-1.38 K if $F_{2\times CO2}$ is assumed to equal 3.7 W/m^2, and 1.15-1.28 K if $F_{2\times CO2}$ equals 3.44 W/m^2, with his preferred model yielding the higher values. Similar values of ECS and TCR have been found by others based on observational data (e.g., see Otto et al. 2013; Richardson et al. 2016; Knutti et al. 2017).

Estimates of ECS and TCR based on climate models tend to be significantly higher than those based on observed data, primarily because climate models predict greater warming than observed in practice (Christy & McNider 2017; Evring et al. 2019; Happer 2019; Zhu et al. 2020). Climate modelers argue that observations do not adequately account for the physics of the

feedbacks and, therefore, "evidence from climate modelling favours values of ECS in the upper part of the 'likely' range [1.5-4.5 K], whereas many recent studies based on instrumentally recorded warming ... favour values in the lower part of the range" (Knutti et al. 2017, p. 731). The 'best-effort' models used in the AR5 report (IPCC 2013) find ECS values in the range 2 K to 5 K, with a best estimate of 3.0 K (Knutti et al. 2017). Later studies by Otto et al. (2013) using an energy balance model (EBM) find an ECS of 2.0 K (range: 1.2-3.9 K) and TCR of 1.3 K (0.9-2.0 K) for the first decade of the 21st Century, lower than previous estimates for the 1990s (1.6 K) and the 1970-2007 period (1.4 K), while Phillips et al. (2020) find a best estimate of 2.05 K. Based on simulations from an ensemble of climate models developed under the Coupled Model Inter-comparison Project (known as CMIP5), Richardson et al. (2016) calculate a TCR value of 1.34 K (0.8-2.6 K) for a mixed layer; they do not attempt to calculate ECS values. The CMIP6 ensemble of climate models prepared for the forthcoming Sixth Assessment Report (AR6) employ unrealistically high values of ECS, which result in warming that does not track with paleoclimate data (Monckton 2019; Zelinka et al. 2020; Zhu et al. 2020; McKitrick & Christy 2020).

Molecular physicists have used the HITRAN database to estimate much lower values of ECS. The reason is that CO_2 molecules can only absorb outgoing radiation of certain wavelengths. Given limitations of the wavelengths, the CO_2 in the atmosphere eventually gets 'saturated' and the extent to which additional atmospheric CO_2 can absorb further radiation is limited (Schildknecht 2020; van Wijngaard and Happer 2020). This is evident in Figure 1, which provides the wavelengths are which atmospheric CO_2 would absorb outgoing radiation and the available radiation to absorb at those wavelengths. Further, the wavelengths that are absorbed methane (natural gas) are the same as those of water vapor, with the result that methane emissions are not likely to be a major contributor to climate warming (van Wijngaard and Happer 2019). Thus, it is

not surprising that Smirnov (2020, p.194), for example, provides an estimate of ECS of 0.6±0.3 ºC. Later he suggests a value of 2.1±0.4 K, "but in this case other reasons than those connected with CO_2 molecules are responsible for the global temperature change" (p.195).

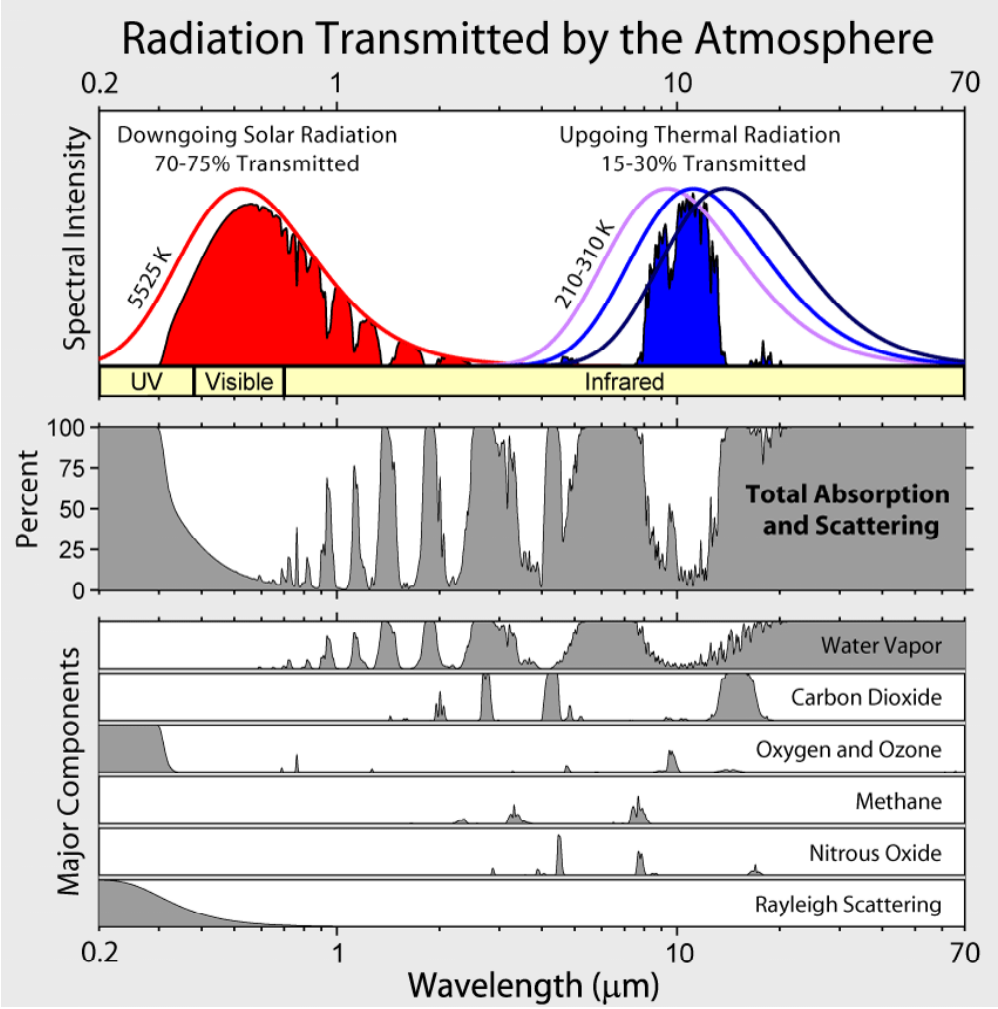

Figure 1: Wavelengths at which gases absorb outgoing infrared radiation. Notice that less radiation occurs (top panel) at the wavelengths absorbed by CO_2 (CO_2 panel)[18]

[18] This figure was provided by William Happer and found at https://www.researchgate.net/figure/Absorption-bands-in-the-Earths-atmosphere-created-by-greenhouse-gases-and-the-resulting_fig8_265041566.

3. NUMERICAL MODELING OF CLIMATE CHANGE

In this section, we consider three different climate models that can be used in the DICE model, but only describe in detail the current model used in DICE. One model we consider essentially has zero dimension because it treats the atmosphere, oceans and terrestrial systems as a single unit. It constitutes a simple energy-balance model (EBM) because it identifies the heat reaching Earth and that subsequently escaping back to space. Any change in the difference between incoming and outgoing radiation constitutes a radiative forcing that, if positive (negative), increases (lowers) the Earth's mean temperature. A second model separates the atmosphere and upper component of the ocean from the deeper ocean, with carbon and heat transferred from the atmosphere/upper ocean to the deep ocean, and vice versa. Given a particular radiative forcing, it could take many years, ranging from decades to centuries, for the two-layer system to get back into equilibrium. Finally, a third variant of the EBMs is used in the DICE model. It has three layers—the atmosphere, an upper ocean layer and a deep ocean layer, with exchanges of carbon dioxide and heat occurring across the boundaries between each of the adjacent layers. Again, it could take many years for the system to come into equilibrium once it is disturbed.

Extremely large and complicated global climate models separate the globe into grids of varying size (e.g., grids that are 2.5° latitude × 2.5° longitude, or one that are measured as 5 km × 5 km, or any other mesh size), with each grid including many atmospheric and ocean layers.[19] Transfers of carbon and heat among grids and layers are modeled. The terrestrial component of the Earth is also included in such models, with heat transfers dependent on the landscape (types of vegetation, land uses, terrain, etc.). Such models also examine energy balances, with exchanges across boundaries dependent on various parameters that are not based on known physical relations

[19] An excellent overview of climate models for the layperson is provided by Koonin (2021, Chapter 5).

and often not explicitly identified. For example, climate modelers must make assumptions about the lapse rate—the rate at which temperature falls with altitude; the lapse rate is affected by radiation, convection, condensation and other factors, and is therefore highly variable. Likewise, little is known about cloud formation and whether and when clouds exacerbate or suppress warming caused by anthropogenic emissions of greenhouse gases.

A simple energy-balance model is just as capable of predicting future trends in global average surface temperatures as a more-complicated global climate model (which also looks at energy balances). Even with a simple energy-balance model (EBM), assumptions need to be made regarding four parameters that are found in all climate models. In some cases, the assumptions are directly modelled via one or more mathematical equations, but they remain assumptions nonetheless. The model parameters that are to be specified are:

1. the depth of the ocean layer assumed to impact heat storage;
2. the transfer of heat between the ocean and the atmosphere;
3. the feedback parameters determining whether, when temperatures rise as a result of some forcing, the warming is exacerbated (positive feedback) or suppressed (negative feedback); and
4. the starting point—the initial temperature departure from the norm (i.e., the temperature anomaly), which affects the sequence of temperature projections from a climate model because, without additional forcing, temperatures should trend toward the norm.

The values of these parameters are not known with certainty, but yet have a profound effect on outcomes.

Simple EBMs are employed by economists (Calel and Stainforth 2017). Figure 2 shows the energy balance for single-layer and two-layer climate models. The DICE model, on the other hand, employs three layers—the atmosphere, an upper ocean layer, and a lower or deep ocean layer. To link the carbon and temperature components in climate models, it is necessary to determine the impact that changes in CO_2 emissions have on the anthropogenic forcing in equations (6) and (7). We begin by describing a simple, one-layer energy balance model.

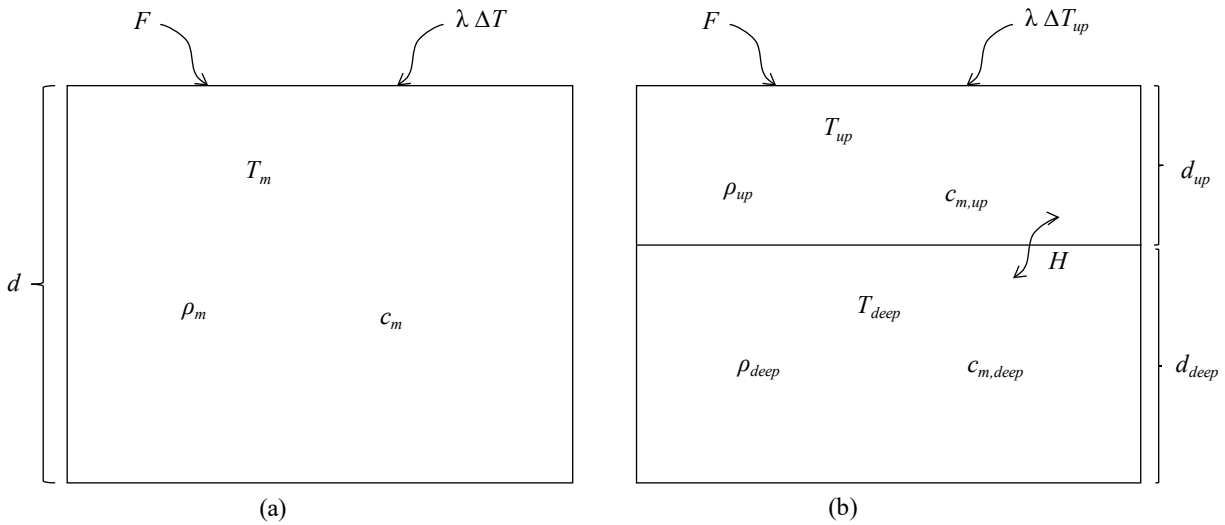

Figure 2: (a) Single Layer Climate Model (b) Two-Layer Climate Model

Zero-dimensional, Single-layer Energy Balance Model

The single-layer or zero-dimensional climate model is given by the energy balance equation (7), which we rewrite in Euler's discrete form as:

$$T_{m,t+1} - T_{m,t} = (\Delta t / C_A)\,(F_t - \lambda\, T_{m,t}), \tag{11}$$

where Δt is the time step (measured in seconds). Consider how equation (11) evolves over time. Suppose we have a starting temperature anomaly given by $T_{m,0}$. For C_A=3.1403 × 10^8 J · K^{-1} · m^{-2}, an ocean depth of 75 m and an annual time step (86,400 s · day^{-1} × 365 days), we rewrite (13) as $T_{m,t+1} - T_{m,t} = 0.100424 \times (F_t - \lambda\, T_{m,t})$.[20] Then, given a forcing F and feedback λ, the temperature anomaly evolves on an annual time step as follows:

Period 1: $T_{m,1} = T_{m,0} + 0.100424 \times [F_0 - \lambda\, T_{m,0}]$
Period 2: $T_{m,2} = T_{m,1} + 0.100424 \times [F_1 - \lambda\, T_{m,1}]$
…
Period N: $T_{m,N} = T_{m,N-1} + 0.100424 \times [F_{N-1} - \lambda\, T_{m,N-1}]$

The change (increase or decrease) in temperature after N years is therefore given by $T_{m,N}$.

[20] In DICE version 2016R2-083017, Nordhaus' parameter $c_1 = 1/C_{AO} = 0.1005$.

It is clear from the above discussion that there are four parameters that drive this simple climate model: (1) the starting value of the temperature anomaly $T_{m,0}$ (which might be zero); (2) the assumed ocean depth; (3) the externally prescribed change in the net radiative plus non-radiative flux (F), which includes an assumption about the initial or current CO_2 forcing to which the projected increase in CO_2 forcing is added; and (4) the total feedback (in essence, the value of λ).

Two-layer Energy Balance Model

Now consider a climate model with two components—an upper mixed atmosphere-ocean layer and a deep ocean. We then rewrite equation (7) so that it includes the heat exchange, denoted by H, between the mixed upper layer and the lower deep-ocean layer:

$$Q_{AO} = C_{AO} \frac{dT_{AO}}{dt} = F - \lambda\, T_{AO} - H, \tag{12}$$

where Q_{AO} is the change in the heat content of the mixed upper (atmosphere-ocean) layer relative to the steady state, and where, as previously, F denotes the radiative forcing and λT_{AO} the outgoing long-wave radiation due to feedbacks.[21] The change in the heat content of the lower (deep-ocean) layer, denoted Q_d, is given by:

$$Q_d = C_d \frac{dT_d}{dt} = H = \beta\,(T_{AO} - T_d), \tag{13}$$

where C_d and T_d are the heat capacity and temperature of the deep ocean, respectively; and β is a parameter relating to the transfer of heat between the upper and lower components. In the case of a single layer model (SLM), $\beta = 0$.

Using observed data, Pretis (2020) estimated the key parameters for implementing the model described by equations (12) and (13). These are summarized in Table 3 for different

[21] Note that C_{AO} is measured as W · yr · m^{-2} · K^{-1} and $\frac{dT_{AO}}{dt}$ as K · yr^{-1}, so Q and H are measured in terms of W per m^2. See also Table 3.

regression models. Depending on the regression model used, Pretis (2020) found λ to be between 2.21 and 2.71 W · K^{-1} · m^{-2}.[22] The global anthropogenic radiative forcing between 1750 and 2011 is estimated to be 2.29 W · m^{-2} (range: 1.1-3.3 W · m^{-2}) (IPCC 2013, p.696), while temperature has risen about 1.0 K, which implies λ = 2.29 W · m^{-2} · K^{-1}, well within the range estimated by Pretis (2020). These values, along with those of ECS and TCR provided earlier, are used in the climate models developed in the next section. In the DICE model, for example, $\lambda = \frac{F_{2\times CO_2}}{ECS}$; if $F_{2\times CO2}$ = 3.7 W · m^{-2} and ECS = 3.1ºC, then λ = 1.194 W · K^{-1} · m^{-2}; for $F_{2\times CO2}$ = 3.44 W · m^{-2} and ECS = 1.5ºC, λ = 2.29 W · K^{-1} · m^{-2}.

Table 3: Estimates of Key Climate Model Parameters

	Regression model		
Item	#1	#2	#3
β/C_d	7.82	7.43	7.35
C_d [W · yr · m^{-2} · K^{-1}][a]	22.72	24.39	24.39
λ [W · m^{-2} · K^{-1}]	2.71	2.29	2.21
ECS [K]	1.37	1.62	1.67
$F_{2\times CO2}$ (=λ×ECS) [W · m^{-2}][b]	3.71	3.71	3.69

Source: Pretis (2020, p.268).
[a] This is usually measured as [J · m–2 · K–1], where 1 J = 2.4333 W · yr.
[b] This is the TCR value, which is taken as 3.7 or 3.44 W/m2, as noted in the text.

Finally, as the atmospheric concentration of CO_2 rises, the anthropogenic forcing increases as well. The equation that is used in climate models is equation (6), which is repeated here:

$$F_t = F_{2\times CO2} \times \frac{ln\left(\frac{CO_{2,t}}{CO_{2,base}}\right)}{ln(2)}, \quad (6)$$

where $CO_{2,t}$ and $CO_{2,base}$ refer to either the cumulative mass of carbon (measured in Gt CO_2) in the atmosphere at time t and the pre-industrial period (1750 or some other base year), or to the

[22] Alternatively, using HadCRUT4 annual data, $T_m \approx 0.75$ºC from 1971 to 2010, and the overall anthropogenic forcing over this period has been 0.42 W · m^{-2} (Table 2); therefore, $\lambda = F/T = 0.42/0.75 = 0.56$ W · m^{-2} · K^{-1}, which dampens the increase in temperature from anthropogenic forcing.

concentration of CO_2 in the atmosphere (measured in ppm) at t and 1750.

Summaries of the physical parameters that are relevant for the development of climate models are provided in Table 4, along with data from the earlier Tables 1 through 3.[23] In addition to observational data in Table 3, other observational evidence for many of the parameters has also recently come to light. For example, de Larminat (2019) provides information on the feedback parameter and scaling factors used in conjunction with a priori forcings that inform equation (5). He used historic temperature data for the period 1850-2010, and tree-ring and other proxy data for the period 850-2010, to estimate parameter values that differ significantly from those used by the IPCC. These are provided in Appendix Table A.1.

A simple, two-layer box model (TLM) of the ocean-atmosphere employs an upper ocean mixing layer and a deep ocean layer. We can assume that the second (deep-ocean) layer has no energy sources or sinks other than the transfer of energy to/from the upper layer.[24] The TLM can be described by the discretized form of equations (12) and (13) as follows:

$$C_{AO}\,(T_{AO,t+1} - T_{AO,t}) = (F_t - \lambda\, T_{AO,t} - H_t)\,\Delta t, \tag{14}$$

$$C_{deep}\,(T_{deep,t+1} - T_{deep,t}) = H_t\,\Delta t = \beta\,(T_{AO,t} - T_{deep,t})\,\Delta t \tag{15}$$

where C_{AO} and C_{deep} refer to the heat content of the atmosphere-upper-ocean layer (as discussed earlier) and the deep-ocean layer, respectively. The heat content of the deep-ocean component is given by: $C_{deep} = \rho_{deep} \times c_{m,deep} \times d_{deep}$, where ρ_{deep} is the density of water (1,000 kg/m^3), $c_{m,\text{deep}}$ is the specific heat capacity of water (4.187 kJ kg^{-1} K^{-1}), and d_{deep} is the ocean depth. If the deep ocean layer is identified as 75 to 2650 m, then the heat capacity of the deep-ocean layer is C_{deep} = (2650

[23] There are numerous studies that provide information that corroborates the data in Table 4, although there are also many studies that would lead to different parameterizations.
[24] There is a literature indicating that carbon in biomass created by photosynthesis near the surface will sink to the ocean floor, permanently locking up carbon (Buesseler et al. 2020).

– 75) m × 1000 kg/m^2 × 4.187 kJ/(kg K) = 10.782 × 10^9 J · K^{-1} · m^{-2}.

Table 4: Summary of Physical Parameters used in the Climate Models

Description	Parameter	Parameter Values[a]	Units of measurement
Forcing under 2 ×CO_2	$F_{2\times CO2}$	3.7 [3.44]	W · m^{-2}
Carbon content of atmosphere in 1750	$CO_{2,1750}$	2,184.9558	Gt CO_2
Carbon content of atmosphere in 1900	$CO_{2,base}$	2,307.4694	Gt CO_2
Carbon content of atmosphere in 2020	$CO_{2,2020}$	3,238.4166	Gt CO_2
Total carbon content of world oceans		140,000	Gt CO_2
		38,000	Gt C
Average depth of world oceans[b]		2,650	m
Heat content of atmosphere	C_A	10.25 × 10^6	J · K^{-1} · m^{-2}
Heat content of ocean	C_O	d × 4.187 × 10^6	J · K^{-1} · m^{-2}
Heat content of atmosphere plus 150 m of ocean	C_{AO}	638.300 × 10^6	J · K^{-1} · m^{-2}
Equilibrium climate sensitivity (observed)	ECS	2.16 [1.05 – 2.70]	K
Equilibrium climate sensitivity (modeled)	ECS	3.1 [1.5 – 6.0]	K
Transient climate response	TCR	1.34 [0.8 – 2.6]	K
Time step (one year)	Δt	31.536 × 10^6	s
Heat transfer coefficient from atmosphere to ocean[b]	β	0.66 (0.0088)	W · m^{-2} · K^{-1}
Slope of thermocline in upper ocean layer[c]		-0.03057	K · m^{-1}
Slope of thermocline in deep ocean layer[c]		-0.00190	K · m^{-1}

[a] Alternative values or range of values provided in square brackets; d refers to depth of ocean.
[b] See https://worldoceanreview.com/en/wor-1/ocean-chemistry/co2-reservoir/ [accessed June 5, 2020]. $\beta = H/\Delta T$ where H is the heat flux (W· m–2) and ΔT is the difference between the surface temperature and that of the ocean layer. Levitus et al. (2012) indicate a warming rate H of 0.27 W/m2 with ocean temperature change in the top 700 m of 0.18oC, so $\beta = 1.5$.
[c] Some studies assume a surface ocean layer of 1,000 m depth (equaling 50 million km3 water) with temperature falling from 22oC to 6oC; a thermocline for the 1,000 to 4,500 m layer (460 mil km3 water) of 6oC to 2oC; and a deep ocean layer below 4,500 m (890 mil km3) with temperatures from 2oC to 0oC.
Source: See text for description and calculation of parameters.

Finally, H_t is the heat transfer from the atmosphere-upper-ocean layer to the deep-ocean layer during period t; it is proportional to the temperature difference between the atmosphere-upper ocean and the deep ocean, where proportionality refers to the 'conductivity' of the upper ocean. If H_t is negative, heat is transferred from the lower to the upper layer. In the model, CO_2 emissions (and mitigation of emissions or removals of CO_2 from the atmosphere) affect the forcing F_t as discussed previously.

Three-layer Energy Balance Model: Climate in DICE

The DICE model employs a slightly different structure than that represented by equations (14) and (15). It takes the energy balance and separates it into two components, the carbon cycle (Figure 3)

and the temperature component (Figure 4). To link the carbon and temperature components in the climate models, it is necessary to determine the impact that changes in CO_2 emissions have on the anthropogenic forcing in equation (7). Using data from NOAA (2018), we calculate the slope of the thermocline in Figure 4 for the upper ocean with a depth of 75 m to be –0.03057ºC per m of depth, whereas the slope is –0.0019 ºC per m of depth from 75 m to well over 3,000 m.

In the DICE model, the geophysical, carbon-climate equations consist of a carbon module and a temperature module (Nordhaus 2013, 2017, 2018a; Calel and Stainforth 2017). The difference between a simple two-layer model and the model employed in DICE is evident upon comparing Figure 2 with Figures 3 and 4, which provide, respectively, the carbon and temperature-energy components found in DICE. In describing the DICE climate model, we follow Nordhaus' specification.

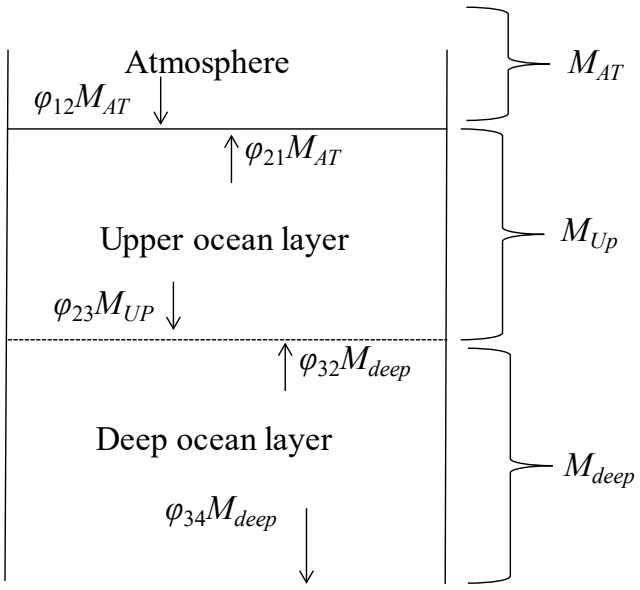

Figure 3: Carbon Cycle in the DICE Model (M refers to carbon)

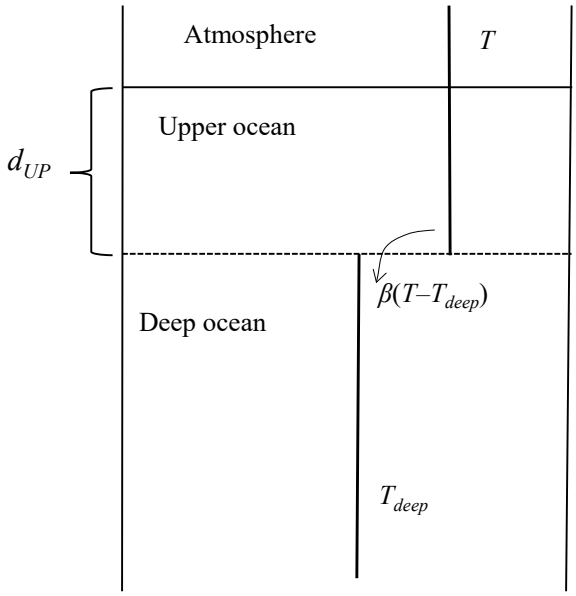

Figure 4: Temperature Component in the DICE Model

Carbon Cycle in DICE Model

Consider a climate system consisting of an atmosphere (denoted by A), upper ocean (U) and deep (lower) ocean (D). We can write the carbon flux equations for each component of the system in terms of its carbon sources and sinks (and measured in terms of Gt CO_2).

$$\frac{dM_A}{dt} = e(t) + \psi_{12} M_U - \psi_{21} M_A \tag{16}$$

$$\frac{dM_U}{dt} = \psi_{21} M_A + \psi_{23} M_D - (\psi_{21} + \psi_{12}) M_U \tag{17}$$

$$\frac{dM_D}{dt} = \psi_{32} M_U - \psi_{23} M_D \tag{18}$$

where e(t) is the rate of emissions (Gt $CO_2 \cdot s^{-1}$), and $M_{A,t}$, $M_{U,t}$ and $M_{D,t}$ represent the carbon in the atmosphere, upper ocean and deep ocean reservoirs, respectively. The ψ_{ij} parameters describe the rate of carbon exchange from reservoir i to reservoir j (in s^{-1}), and are equivalent to an inverse timescale. In the absence of any sources, the integrated solution for carbon in a given reservoir is simply an exponential decay with e-folding timescale of $\tau_{ij} = 1/\psi_{ij}$. This can also be interpreted as a 'residence time' of carbon in the various reservoirs (layers), which is a common concept in the

earth sciences.[25]

Integrating the discretized equations (16) through (18) enables us to represent the carbon cycle in Figure 3 in the equations given by Nordhaus:

$$M_{A,t} = E_{t-1} + (1 - \varphi_{12})\, M_{A,t-1} + \varphi_{21}\, M_{U,t-1} \tag{19}$$

$$M_{U,t} = (1 - \varphi_{21} - \varphi_{23})\, M_{U,t-1} + \varphi_{12}\, M_{A,t-1} + \varphi_{32}\, M_{D,t-1} \tag{20}$$

$$M_{D,t} = (1 - \varphi_{32})\, M_{D,t-1} + \varphi_{23}\, M_{U,t-1} \tag{21}$$

For a given carbon reservoir, M_R, $R=\{A, U, D\}$, $M_{R,t}$ is the total carbon in a given reservoir at time t, and $M_{R,t-1}$ and E_{t-1} are the reservoir values and total emissions in the previous time step. For a timestep, Δt, $\varphi_{ij} = \psi_{ij}\Delta t$ is the fraction of carbon transferred between reservoirs, while $(1 - \varphi_{ij})$ represents the proportion of carbon that is retained to the next period. Note that $0 \leq \varphi_{ij} \leq 1$, $\forall i,j$. The values of the parameters used in the current study and those used in earlier versions of DICE are found in Table 5, with the retention terms written as φ_{ii} in Nordhaus' notation.[26] Note that the φ_{ij} values must be scaled by Δt when using different model time steps; however, ψ_{ij} values are independent of the timestep used.

Temperature Module in DICE

In the DICE model, the temperature flux between the atmosphere and deep ocean depends on the gradient in the upper ocean (as shown in Figure 4) and thereby the depth of the upper ocean. The temperature in each period is given by the following equations:

$$T_t = T_{t-1} + \frac{\Delta t}{C_{up}} \left[F_{t-1} - \lambda\, T_{t-1} - \beta\, (T_{t-1} - T_{t-1}^{deep})\right] \tag{22}$$

[25] Note that these should be easier to find and define than Nordhaus' proportional transfer coefficients as residence times are commonly estimated in the literature.

[26] These values do not need to be defined, as they are simply equal to $(1 - \sum_{j \neq i} \varphi_{ij})$.

$$T_t^{deep} = T_{t-1}^{deep} + \frac{\beta \Delta t}{C_{deep}} (T_{t-1} - T_{t-1}^{deep}) \quad (23)$$

where T is the increase in atmospheric temperature in ºC since pre-industrial times; $\lambda = \frac{F_{2\times CO_2}}{ECS}$; T^{deep} is the increase in lower ocean temperature in ºC since 1750; and F_t is the increase in radiative forcing (W/m^2) from 1750 in period t. The value of $F_{2\times CO2}$ is taken to be 3.44 W/m^2 or, more often, 3.7 W/m^2 (with Nordhaus using 3.6813 in DICE v2016R), while ECS is set to a value between 1.5 and 4.5 K.

Table 5: Parameter Values used in the DICE Model, Past and Current

Parameter	DICE 2016R2	DICE 2013	DICE 2008	Current
		General		
$F_{2\times CO2}$	3.6813	3.8	3.8	3.7
ECS	3.1	2.9	3.2	2.0
		Damage function		
a_1 (intercept)	0	0	0	
a_2 (quadratic term)	0.00236	0.00267	0.0028388	
a_3 (exponent)	2.0	2.0	2.0	
		Carbon module		
φ_{11}	0.88	0.912	0.810712	0.9
φ_{21}	0.12	0.088	0.189288	0.1
φ_{12}	0.196	0.052267	0.097213	0.0033
φ_{22}	0.797	0.945233	0.852787	0.9917
φ_{32}	0.007	0.0025	0.05	0.0050
φ_{23}	0.11433	0.038329	0.003119	0.0015
φ_{33}	0.98857	0.961671	0.996881	0.9975
		Temperature module[a]		
$c_1 = \frac{\Delta t}{C_{up}}$	0.1005	0.098	0.208	(3.0767, 0.0973)[b]
β	0.0880	0.088	0.31	0.008 [1.3]
$c_2 = \frac{\beta \Delta t}{C_{deep}}$	0.0250	0.025	0.05	0.00034

[a] The parameters are as follows: $c1$ is the adjustment speed of the atmospheric temperature; β is the heat loss from the upper ocean & atmosphere to the deep ocean; and $c2$ is the coefficient representing the heat gain by the deep ocean.
[b] The two values depend on (CA, CAO) from Table 3 and use a one-year time step.
Source: Calel and Stainforth (2017) and authors' calculations from various DICE models.

Equations (22) and (23) are similar to (14) and (15), with the variables and parameters in the above equations defined earlier. The heat content of the atmosphere is given by C_A, as described

earlier, and is provided in Table 3. If the depth of the upper ocean is taken to be 75 m, then the heat capacity of the upper ocean layer would be C_{up} = 75 m × 1000 kg/m^3 × 4.187 kJ/(kg K) = 314.025 × 10^6 J · K^{-1} · m^{-2}. For the deep ocean of 2,650 m, the heat capacity would be C_{deep} = (2650 – 75) m × 1000 kg/m^3 × 4.187 kJ/(kg K) = 10,781.525 × 10^6 J · K^{-1} · m^{-2}. Values of the forgoing parameters used in various DICE models and the current study are also found in Table 5.

Here parameter β is the heat transfer coefficient (W m^{-2} K^{-1}), describing the efficiency of energy transfer between the atmosphere and deep ocean through the upper ocean. Nordhaus used a value of 0.31 W m^{-2} K^{-1} in DICE 2008, and a value of 0.088 W m^{-2} K^{-1} in subsequent models, while Gregory and Mitchell (1997) use a larger value of 0.66 W m^{-2} K^{-1} in their application of the DICE model. It is not immediately clear how these values were obtained.

As with ψ_{ij} above, we can also determine a timescale for thermal mixing. From simple dimensional analysis of Equations (22) and (23), we see that

$$\tau_T = \frac{C_R}{\beta}. \tag{24}$$

is the (mixing) timescale for heat within a given reservoir R with a heat capacity, C_R. Calculating the value of τ_T for the upper and deep ocean layers using the 2016R2 parameters in Table 5, this gives us an upper ocean timescale of ~113 years, and a deep ocean timescale of ~3000 years. Both are reasonable for ocean values (though the upper ocean is generally faster, but that is due to it being a thinner layer than 75 m); therefore, β can be defined according to the mixing timescale.

Climate Model Projections

NASA indicates that global mean temperature will increase by 1.8ºC to 4.0ºC during the 21st Century.[27] The rise in temperatures will depend on the RCP scenario that is chosen. Four available

[27] See https://scied.ucar.edu/longcontent/predictions-future-global-climate [accessed June 9, 2020].

RCP scenarios are provided in Figure 5. Scenarios indicate by how much CO_2 emissions are projected to increase above average emissions in 1990—the Kyoto Protocol baseline. The most pessimistic scenario (RCP8.5) has emissions increasing continuously so that they exceed baseline emissions by nearly 29 Gt CO_2, while the most optimistic scenario (RCP2.6) has emissions rising to a maximum of 10.3 Gt CO_2 in 2020 and then falling throughout the rest of the 21st Century, with reductions in global emissions beginning in 2080. Although many studies treat the RCP8.5 scenario as business as usual, global emissions are already lower than projected; RCP8.5 assumes that "coal accounts for half of future carbon-dioxide emissions through 2100, and two-thirds of the emissions through 2500" (Rutledge 2014). This pathway should not be considered and certainly not as a business-as-usual scenario (Hausfather and Peters 2020). Further, each scenario is considered to be as likely to occur as any other. Figure 6 shows the projected concentrations of atmospheric CO_2 for each of the four RCP scenarios.

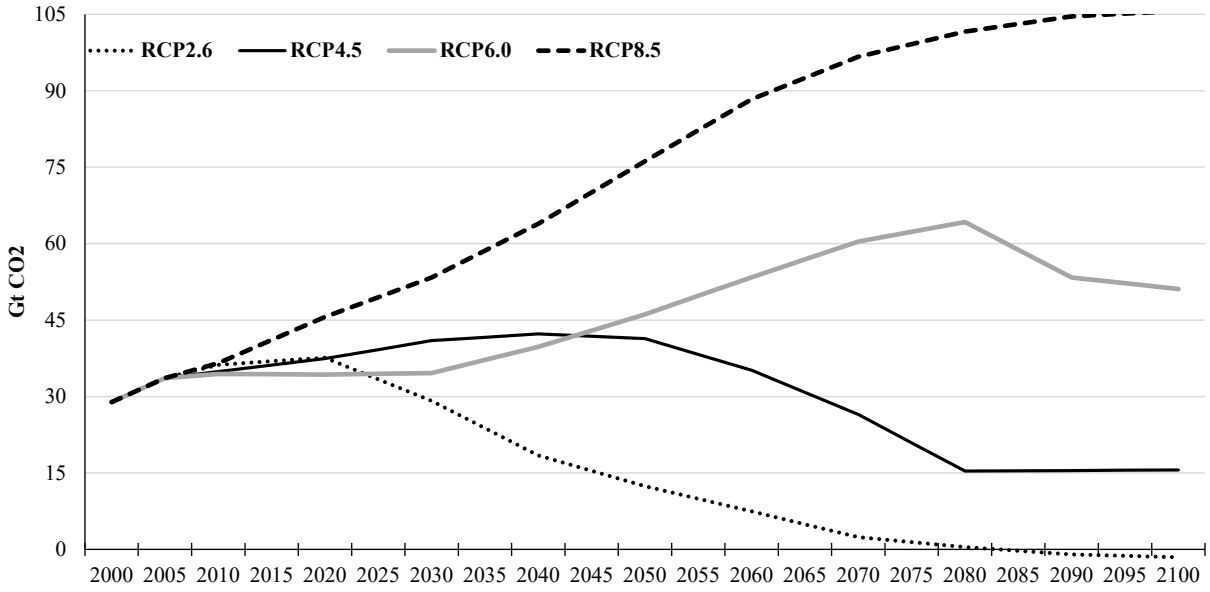

Figure 5: Projected Annual Emissions of CO_2 under Four Representative Concentration Pathways (RCP)

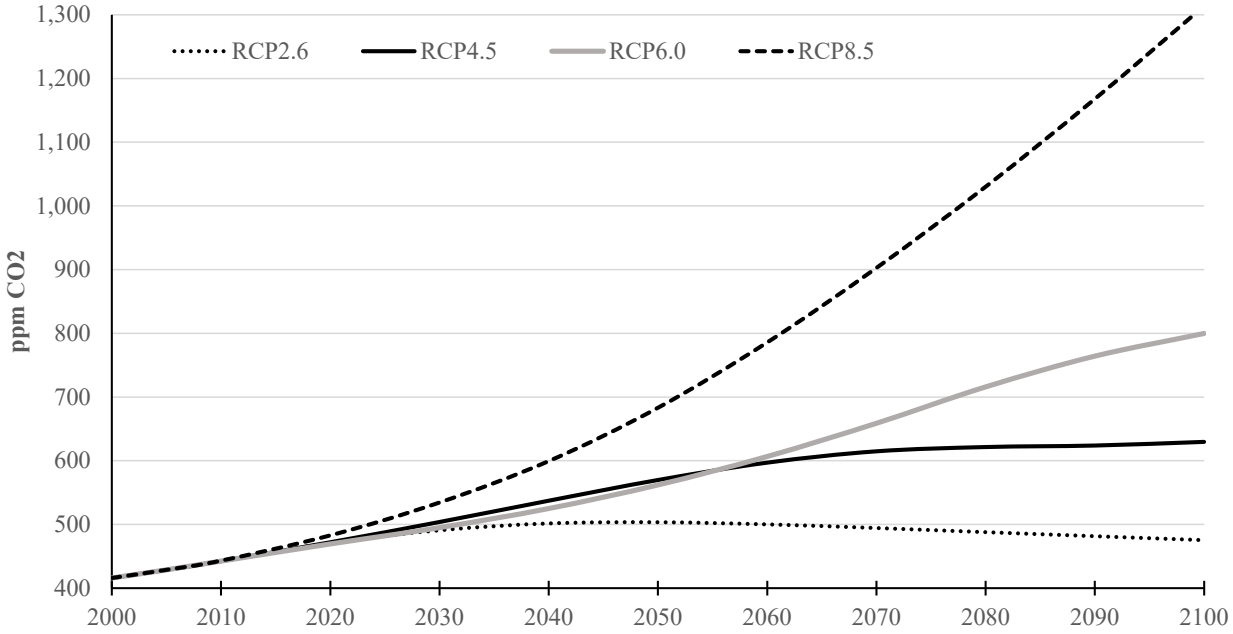

Figure 6: Projected Concentration of Atmospheric CO_2 under Four Representative Concentration Pathways (RCP)

We can project different temperature scenarios for the RCP scenarios using the DICE model and compare it to the projections from the CMIP5 ensemble.[28] These are provided in Figure 7. The temperature projections suggest that the DICE model is running a bit hot compared to the large climate models used by the IPCC.

[28] We also have temperature projections for the SLM and TLM models, but, at this time with the parameterization indicated in Tables 2 and 4 and the earlier discussion, these are quite a bit higher than the projections from DICE and the CMIP5 ensemble. Note, for example, that the average of the CMIP5 models is twice as large as observed temperatures since 1979; only the Russian INM-CM4 (Institute for Numerical Mathematics–Climate Model Four) predicts the least warming, tracking observed temperatures quite well.

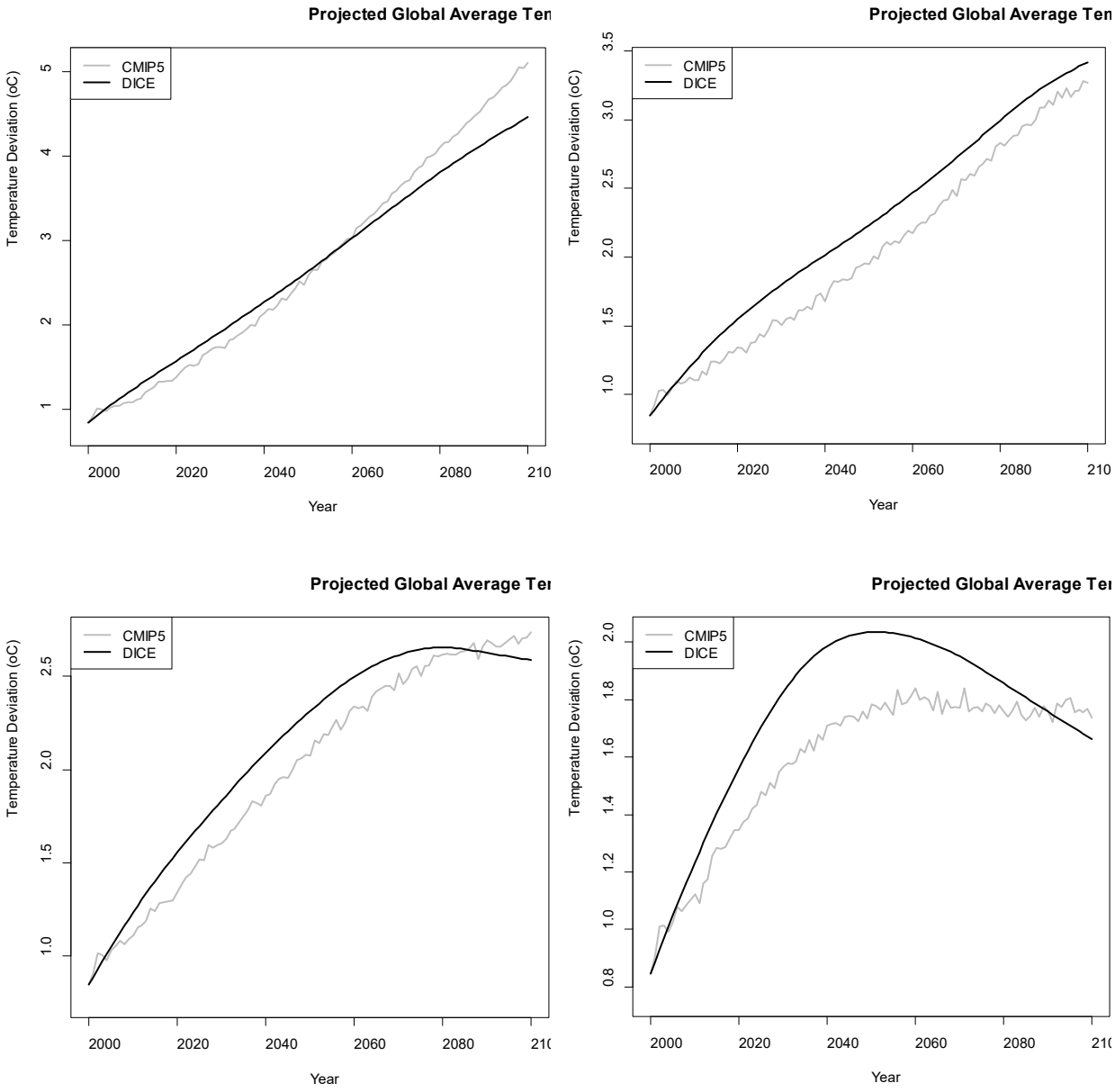

Figure 6: Projected Temperatures: A Comparison of DICE Model Outcomes vs. CIMP5 Averages, Four Representative Concentration Pathways

4. DICE MODEL

The objective of the DICE model (Nordhaus 2013, 2017, 2018a,b) is to maximize the future discounted flow of social wellbeing subject to a set of constraints. The future flow of social welfare W is expressed as the discounted sum over future time periods of the population-weighted utility of per capita consumption (Nordhaus 2018b; p. 336):

$$W = \sum_{t=1}^{T_{max}} U(c_t, L_t) r_t \tag{25}$$

where U is utility; L is population; c is per capita consumption ($c = C/L$ where C denotes aggregate consumption); r is the discount factor, $r_t = (1+\rho_t)^{-t}$, where ρ_t is society's consumption discount rate that weights the utilities of future generations but changes according to the Ramsey discounting formula (van Kooten 2021, pp.41-46); and t refers to time (where DICE employs a five-year time step, but we consider a one-year time step as well). The aggregate utility function employed by Nordhaus (Nordhaus 2018b, p.336) is defined as:

$$U(c_t, L_t) = L_t \left[c_t^{(1-\alpha)}/(1-\alpha)\right], \tag{26}$$

where $c_t^{(1-\alpha)}/(1-\alpha)$ is per capita utility, and α is the constant elasticity of the marginal utility of per capita consumption, which represents the extent to which consumption is substitutable across time or, more pertinently, across different generations.

If α is close to zero, the consumption of one generation and another are close substitutes; if α is high, they are not close substitutes. The coefficient α thus also represents a measure of relative Intergenerational Inequality Aversion (IIA). Rezai and van der Ploeg (2016), whose IAM uses a utility function of the same general form as (26), provide a good discussion of this coefficient and its relation to a carbon tax. As additionally discussed in Kverndokk et al. (2013, p.4), who in turn cite Heal (2009), the value of α may influence climate change mitigation decisions in two ways. First, in terms of intergenerational equity, a higher value for α means that if

consumption is predicted to rise over time, the decision maker will assign a lower weight to the utility of future generations due to a higher aversion to future generations becoming wealthier than the present. Second, there is an implication for intra-generational equity. If the value for α is high (i.e., future generations valued less), then the decision maker will tend to undertake less climate change mitigation and poor nations are likely to suffer more from that choice than are wealthier countries.

In their baseline analysis, Rezai and van der Ploeg (2016, p. 505) employ a "widely used" value of 2.0 for IIA (α in (26), φ in their notation), but they also use values of IIA = 1.0 to convey the importance of this parameter in terms of its implications for determining an optimal carbon tax. The DICE model uses a value of α = 1.45 (Nordhaus 2018b, p. 336). In his 2016 assessment of the implications of various sources of uncertainty in DICE, Nordhaus does not include the discount rate (of which, based on the Ramsey formula, IIA is one component) as an uncertain variable and acknowledges that "generational preferences are uncertain and might evolve differently over time. Uncertainties about preferences pose philosophical difficulties that are not easily represented in economic growth models and are therefore excluded" in that particular assessment of DICE (Nordhaus 2018b, p. 342).

Note that the per capita utility function actually used in the DICE model differs from that shown in (26) and is:

$$u(c_t) = \{[c_t^{(1-\alpha)} - 1]/(1-\alpha)\} - 1, \qquad (27)$$

which is the standard isoelastic (or constant relative risk aversion) utility function (Norstad 2011) given by $u(c) = [c^{(1-\alpha)} - 1]/(1-\alpha)$, plus an additive term (–1). The practical result of subtracting one from the standard isoelastic utility function is that $u(c=1)$ becomes –1 instead of zero and u is reduced by a value of one for all other values of c.

Net output is specified as gross output minus damages and abatement costs or, employing variable notation slightly different from Nordhaus:

$$Y_t = (1 - \Lambda_t)(1 - D_t)\, B_t\, K_t^{\gamma}\, L_t^{(1-\gamma)}, \tag{28}$$

where Y_t is output net of damages and abatement at time t; Λ_t represents the fraction of output devoted at time t to reducing emissions of CO_2; D_t denotes climate change damages as a fraction of output; B_t is total factor productivity; K_t is capital stock and services; and L_t is labor. Nordhaus implicitly assumes that population and labor are the same, so that per capita consumption needs to be considered as consumption per worker (see Nordhaus 2018b, pp.336-337). The capital stock changes over time according to

$$K_t = I_t + (1-\delta_K)\, K_{t-1} \tag{29}$$

where I_t is the rate of investment in capital stock in period t and δ_K is the rate of capital depreciation. The following then holds as an accounting identity:

$$Y_t = C_t + I_t\,. \tag{30}$$

In the DICE model, climate damages at time t are specified as (Nordhaus 2018b, p.338):

$$D_t = d_1\, T_t^{atm} + d_2\, (T_t^{atm})^2, \tag{31}$$

where we again use slightly different notation than Nordhaus. T_t^{atm} denotes the 'globally averaged temperature change' at time t and the parameters d_1 and d_2 reflect estimated damages as a quadratic function of the change in temperature. Note that, in early DICE specifications, the damage function was expressed as $D_t/(1+D_t)$ to be sure that damages were not greater than economic output. "However, the damage ratio does not approach 1 in the current projections, so the quadratic specification is preferred" (Nordhaus 2018b, p.338).

The fraction of output devoted to reducing emissions of CO_2 at any time is specified as:

$$\Lambda_t = \theta_{1,t}\,\mu_t^{\theta_2}, \tag{32}$$

where it is assumed that $\theta_{1,t} = 0.0741 \times 0.0904^{(t-1)}$ and $\theta_2 = 2.6$ so that, in period 1 if CO_2 emissions are to equal zero, abatement costs would need to equal 7.41 percent of output and that percentage would then decline through time at 2% per period (Nordhaus 2018b, p.337). Several factors follow from (32) and the assumptions pertaining to its parameters. First, since Λ_t is the fraction of output devoted to abatement expenditures, total CO_2 abatement costs are proportional to output Y_t and are an increasing function of the emissions reduction rate u_t, so that total abatement costs at time t are:

$$A_t = \theta_{1,t}\, Y_t\, u_t^{\theta_2}. \tag{33}$$

Second, DICE assumes that a 'backstop technology' exists that can produce energy services at a level of zero greenhouse gas emissions. In that case, μ_t is set equal to one and "the backstop price in 2020 is $550 per ton of CO2-equivalent, and the backstop cost declines at ½ percent per year" (Nordhaus 2018b, p.337). Additionally, DICE assumes that negative emissions energy service production technologies (which would imply $\mu > 1$) are not available in period 1 but would materialize after the year 2150.

Total emissions of CO_2, E_t, are specified as the sum of industrial emissions E_t^{ind}, which are endogenous in the model, and exogenously-determined emissions from land E_t^{land}:

$$E_t = E_t^{ind} + E_t^{land}. \tag{34}$$

Furthermore, uncontrolled industrial CO_2 emissions at time t are assumed to be given by the level of carbon intensity, σ_t, times gross output. Actual (post-control) industrial emissions E_t^{ind} are then reduced according to the emissions reduction rate u_t, and equal:

$$E_t^{ind} = \sigma_t\,(1-u_t)\,B_t\,K_t^{\gamma}\,L_t^{(1-\gamma)}. \tag{35}$$

Additionally, there is an inequality constraint related to the availability of fossil fuels, denoted CC

and which are utilized in industry and thereby produce industrial emissions of CO_2:

$$CC \geq \sum_{t=1}^{T_{max}} E_t^{ind}. \quad (36)$$

The emissions reduction rate, u_t, is the control variable in the model. Nordhaus notes that the level of carbon intensity, σ_t, is also referred to as the CO_2-output ratio and that the historical decline in this ratio on a global scale (as observed at an average negative trend of 1.5% per year since 1960) is termed decarbonization (Nordhaus 2018b, pp.338-339). Therefore, the DICE model assumes that the rate of decarbonization in future periods will be –1.5% annually.

5. External Forcing in DICE: An Application[29]

In this section, we use Nordhaus' DICE model to investigate the economics of restoring 900 million ha of forestlands as proposed by Bastin et al. (2019). They argue that "ecosystem restoration [is] one of the most effective solutions at our disposal to mitigate climate change," and that, by restoring 900 million ha of forested lands, one-quarter of the atmospheric carbon pool could be sequestered in new biomass. In the DICE model, external forcing occurs through changes in land use, with Nordhaus arguing that land use changes (principally deforestation) result in additional CO_2 emissions, although such emissions decline over time as a result of increased conservation. By looking at the most optimistic restoration case, van Kooten (2020) finds that a large terrestrial sink can reduce projected future temperatures by more than 30%, with accompanying smaller marginal damages. It also turns out that optimal levels of industrial emissions increase, thereby reducing the beneficial temperature response of the forestry investment.

One essential change is made to the DICE model. In the DICE model, Nordhaus treats CO_2

[29] The discussion in this section is based on van Kooten (2020).

emissions from land use and land use changes as exogenously determined. He assumes exogenous emissions decline over time. Upon setting exogenous emissions to zero and comparing this to the baseline results, it turns out that the path of optimal marginal damages (as measured by Nordhaus' social cost of carbon, or SCC) is almost unchanged. The SCC of carbon is lower by \$0.35/tCO_2 (\$0.15/tCO_2) in 2100 (2050) when there are no exogenous emissions ($E_{D,t}$=0, $\forall t$) compared to when emissions from deforestation are assumed to occur as noted above [$E_{D,t}$=2.6×(1–0.022)$^{t-1}$ Gt CO_2, t=1, …, 100].

In the analysis, we have $E_{D,t}$ = 900 mil ha × K m^3/ha × 0.2 tC/m^3 × 44 tCO_2/12 tC, where C refers to carbon and K to the value of the mean annual increment (MAI). Upon dividing by 1000, this gives $E_{D,t}$ = 0.660×K Gt CO_2, $\forall t$. In the DICE model, this amount is removed from total emissions in each period. The DICE model then determines the level of industrial emissions in each period so that overall economic welfare across time is maximized.

The results are provided in Figures 7 and 8. These indicate that the restoration of 900 million ha could have a significant impact on future climate damages and optimal emissions from industrial activities. Even in the current model year (2015), restoration of forests could reduce marginal damages by 3.4 (MAI = 2.5 m^3 ha^{-1}) to 18.1 (MAI=10.0 m^3 ha^{-1}) percent. From Figure 7, marginal damages could potentially be reduced by 3.5% to 31.0% by 2050, and by 5.3% to 32.4% by 2100.

The introduction of a large terrestrial carbon sink will, however, concurrently increase the economically optimal level of industrial emissions of CO_2 (Figure 8). This is because the projected rise in temperature is lower with higher levels of timber growth. The projected temperature increase by 2050 of 2.03ºC in the base case falls to 1.90ºC for the low growth scenario to 1.56ºC in the high growth scenario. For 2100, the temperature projections fall from 3.48ºC in the base

case to 3.16ºC and 2.21ºC for the low and high growth scenarios, respectively.

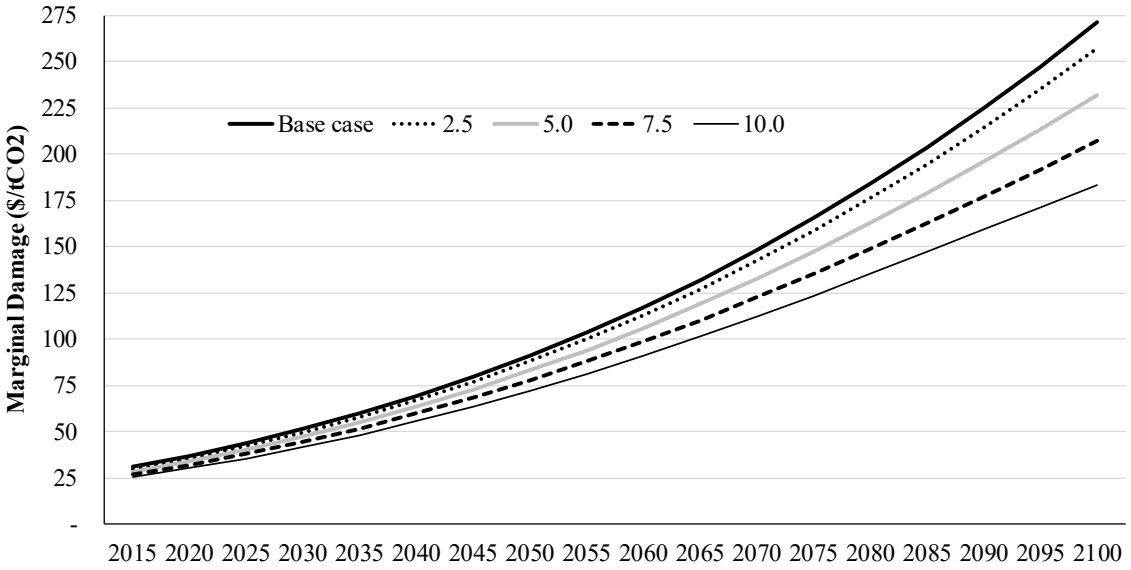

Figure 7: Estimates of the marginal damages (i.e., social cost of carbon) from the DICE (vR2016) model for the base case and four levels of assumed rates of timber growth on 900 million ha, where values indicate the MAI in m^3 ha^{-1}. Source: van Kooten (2020)

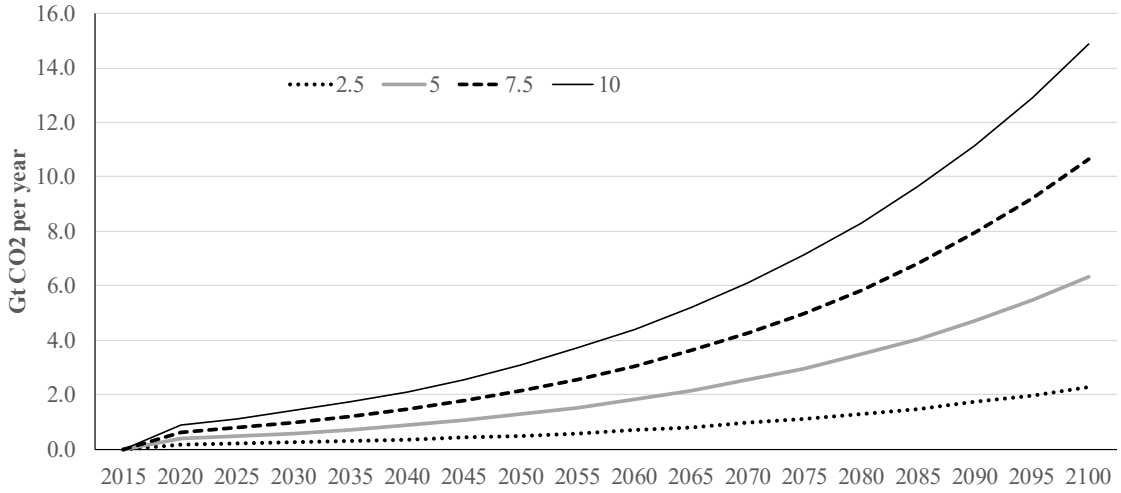

Figure 8: Departure of optimal industrial emissions of CO_2 from baseline emissions for four levels of assumed rates of timber growth (measured by MAI in m^3 ha^{-1}) on 900 million ha, as derived from the DICE (vR2016) model. Source: van Kooten (2020)

6. CONCLUDING DISCUSSION

Policy makers need estimates of the economic damages of global climate change to guide decisions about carbon taxes and assess the benefits of mitigation. Currently, the DICE model is one of the few IAMs available to generate information about the marginal damages from fossil fuel emissions—the social cost of carbon—and thus yields useful outputs for assessing alternative mitigation proposals. At the same time, DICE and other IAMs yield outcomes that are quite sensitive to assumptions regarding parameters that determine linkages between (1) CO_2 emissions and global temperatures, and (2) global temperatures and economic damages. The analyses in this manuscript represent incremental steps toward elucidating the importance of assumptions made in both of these IAM components. The results thus far affirm the sensitivity of climate component outputs to parameter values. Additionally, our climate modelling results indicate that the climate component of the DICE model tracks the CMIP5 ensemble averages quite well for the four RCP scenarios considered here; it appears, indeed, that projections of average global surface temperatures fall well within the band of temperature projections from the climate models comprising the CMIP5 ensemble.

Our primary next steps will be to continue to examine the importance of uncertainty in parameters, with a focus on coefficients that are both highly uncertain as well as key in terms of determining model outputs. In the climate component of the DICE model, one such parameter is the transfer of heat from the atmosphere and upper ('surface') ocean layer to the deep oceans (β). In the economic component, it is necessary to investigate the influence of uncertainty in several parameters. One example is the coefficient α, the measure of intergenerational inequality aversion, which is a component of the social discount rate. The influence of this parameter has not been addressed in the most recent assessment of the impacts of uncertainty in DICE. More broadly, next

steps for future research will involve disentangling the social discount rate for monetary values (goods) from the discount rate used for carbon emissions. The intent will be to inform modellers and policymakers who wish to account for the urgency of mitigation due to the time lags and irreversibilities associated with carbon emission impacts.

7. REFERENCES

Alexander, R.B., 2021. Weather Extremes: Are They Caused by Global Warming? Report 49. 46pp. London: The Global Warming Policy Foundation. Available at: https://www.thegwpf.org/.

Alexander, R.B., 2020. Extreme Weather in 2020. Report 43. 32pp. London: The Global Warming Policy Foundation. Available at: https://www.thegwpf.org/.

Auffhammer, M., 2018. Quantifying Economic Damages from Climate Change, *Journal of Economic Perspectives* 32(4): 33-52. DOI: 10.1257/jep.32.4.33.

Bastin, J.-F., Y. Finegold, C. Garcia, D. Mollicone, M. Rezende, D. Routh, C.M. Zohner and T.W. Crowther, 2019. The Global Tree Restoration Potential, *Science* 365(6448): 76-79. DOI: 10.1126/science.aax0848.

Buesseler, K.O., P.W. Boyd, E.E. Black and D.A. Siegel, 2020. Metrics that Matter for Assessing the Ocean Biological Carbon Pump, *Proceedings of the National Academy of Sciences* 117(18): 9679-9687. doi: 10.1073/pnas.1918114117.

Calel, R. and D.A. Stainforth, 2017. On the Physics of Three Integrated Assessment Models, *Bulletin of the American Meteorological Society* 98: 1199-1216.

Christy, J.R. and R.T. McNider, 2017. Satellite Bulk Tropospheric Temperatures as a Metric for Climate Sensitivity, *Asia Pacific Journal of Atmospheric Science* 53(4): 511-518.

Dahlman, L.A. and R. Lindsey, 2020. Climate Change: Ocean Heat Content, Climat.gov Blog August 17. Available at https://www.climate.gov/news-features/understanding-climate/climate-change-ocean-heat-content [accessed May 7, 2021].

Dayaratna, K., R. Mckitrick and D. Kreutzer, 2017. Empirically Constrained Climate Sensitivity and the Social Cost of Carbon, *Climate Change Economics* 8(2): 1750006. https://doi.org/10.1142/S2010007817500063.

de Laat, A.T.J. and A.N. Maurellis, 2006. Evidence for Influence of Anthropogenic Surface Processes on Lower Tropospheric and Surface Temperature Trends, *International Journal of Climatology* 26: 897-913.

de Laat, A.T.J. and A.N. Maurellis, 2004. Industrial CO_2 Emissions as a Proxy for Anthropogenic Influence on Lower Tropospheric Temperature Trends, *Geophysical Research Letters* 31(5): L05204, doi:10.1029/2003GL019024.

de Larminat, P., 2019. Black Box Identification of Earth's Climate System. https://hal.archives-ouvertes.fr/hal-02178554 [accessed June 15, 2020].

de Larminat, P., 2016. Earth Climate Identification vs. Anthropic Global Warming Attribution, *Annual Reviews in Control* 42: 114-125.

Dut, A., 1998. Mass of the Oceans. The Physics Factbook. An Encyclopedia of Scientific Essays. https://hypertextbook.com/facts/1998/AvijeetDut.shtml [accessed April 17, 2020].

Essex, C. and R.R. McKitrick, 2002. Taken By Storm: The Troubled Science, Policy and Politics of Global Warming Toronto, ON: Key Porter Books.

Eyring, V., P.M. Cox, G.M. Flato, P.J. Gleckler, G. Abramowitz, P. Caldwell, W.D. Collins, B.K. Gier, A.D. Hall, F.M. Hoffman, G.C. Hurtt, A. Jahn, C.D. Jones, S.A. Klein, J.P. Krasting, L. Kwiatkowski, R. Lorenz, E. Maloney, G.A. Meehl, A.G. Pendergrass, R. Pincus, A.C. Ruane, J.L. Russell, B.M. Sanderson, B.D. Santer, S.C. Sherwood, I.R. Simpson, R.J. Stouffer and M.S. Williamson, 2019. Taking climate model evaluation to the next level, *Nature Climate Change* 9(February): 102-110. doi: 10.1038/s41558-018-0355-y.

Frank, P., 2019. Propagation of Error and the Reliability of Global Air Temperature Projections, *Frontiers in Earth Science* 7(September): Article 223. 17pp. doi: 10.3389/feart.2019.00223.

Goklany, I.M., 2021. Impacts of Climate Change: Perception and Reality, GWPF Report 46. London, UK: The Global Warming Policy Foundation. https://www.thegwpf.org/content/uploads/2021/02/Goklany-EmpiricalTrends.pdf [accessed May 19, 2021].

Gregory, J.M. and J.F.B. Mitchell, 1997. The climate response to CO2 of the Hadley Centre coupled AOGCM with and without flux adjustment, *Geophysical Research Letters* 24 (15), August: 1943-1946. DOI: 10.1029/97GL01930.

Happer, W., 2019. Happer's Statement: CO_2 will be a Major Benefit to the Earth. Focused Civil Dialogue on Global Warming. November 20. The Best Schools. https://thebestschools.org/special/karoly-happer-dialogue-global-warming/happer-major-statement/ [accessed April 16, 2020].

Hartmann, D.L., 2016. *Global Physical Climatology, 2nd Edition*. 498pp. Elsevier.

Hausfather, Z. and G.P. Peters, 2020. Emissions – the "Business as Usual" Story is Misleading, Nature 577: 618-620. 29 January. https://www.nature.com/articles/d41586-020-00177-3 [accessed May 7, 2021].

Heal, G., 2009. Climate Economics: A Meta-Review and Some Suggestions for Future Research, Review of Environmental Economics and Policy 3(1): 4-21.

Hope, C., 2006. The Marginal Impact of CO_2 from PAGE2002: An Integrated Assessment Model Incorporating the IPCC's Five Reasons for Concern, *The Integrated Assessment Journal* 6(1): 19-56.

Hourdin, F., T. Mauritsen, A. Gettelman, J. Golaz, V. Balaji, Q. Duan, D. Folini, D. Ji, D. Klocke, Y. Qian, F. Rauser, C. Rio, L. Tomassini, M. Watanabe and D. Williamson, 2017. The Art and Science of Climate Model Tuning, *Bulletin of the American Meteorological Society* March: 589-602. doi:10.1175/BAMS-D-15-00135.1.

Hoven, R., 2012. NASA's Rubber Ruler, *American Thinker* September 25. At https://www.americanthinker.com/blog/2012/09/nasas_rubber_ruler.html#ixzz27YZRxqIW [accessed May 7, 2021].

IPCC, 2013. *Climate Change 2013: The Physical Science Basis. Contribution of Working Group I to the Fifth Assessment Report of the Intergovernmental Panel on Climate Change* [Stocker, T.F., D. Qin, G.-K. Plattner, M. Tignor, S.K. Allen, J. Boschung, A. Nauels, Y. Xia, V. Bex and P.M. Midgley (eds.)]. Cambridge University Press, Cambridge, United Kingdom and New York, NY, USA, 1535 pp.

IPCC, 2007: *Climate Change 2007: The Physical Science Basis*. *Contribution of Working Group I to the Fourth Assessment Report of the Intergovernmental Panel on Climate Change* edited by S. Solomon, D. Qin, M. Manning, Z. Chen, M. Marquis, K.B. Averyt, M. Tignor and H.L. Miller. Cambridge, UK: Cambridge University Press.

IPCC, 2001. *Climate Change 2001: The Scientific Basis*. *Contribution of Working Group I to the Third Assessment Report of the Intergovernmental Panel on Climate Change* edited by J.T. Houghton, Y. Ding, D.J. Griggs, M. Noguer, P.J. van der Linden, X. Dai, K. Maskell, and C.A. Johnson. Cambridge, UK and New York, NY: Cambridge University Press. 881pp.

Johnston, C.M.T. and G.C. van Kooten, 2015. Back to the Past: Burning Wood to Save the Globe, *Ecological Economics* 120(December): 185-193.

Khilyuk, L.F. and G.V. Chilingar, 2006. On Global Forces of Nature Driving the Earth's climate. Are Humans Involved? *Environmental Geology* 50(6): 899-910. doi: 10.1007/s00254-006-0261-x

Knutti, R., M.A.A. Rugenstein and G.C. Hegerl, 2017. Beyond Equilibrium Climate Sensitivity, *Nature GeoScience* 10(October): 727-736. doi: 10.1038/NGEO3017.

Koonin, S.E., 2021. *Unsettled. What Climate Science Tells Us, What is Doesn't, and Why it Matters*. Dallas, TX: BenBella Books.

Koutsoyiannis, D., 2021. Rethinking Climate, Climate Change, and Their Relationship with Water, *Water* 13(6): 849. https://doi.org/10.3390/w13060849.

Kverndokk, S., E. Naevdal and L. Nøstbakken, 2013. The Trade-off between Intra- and Intergenerational Equity in Climate Policy. CESifo Working Paper No. 4285, Category 10: Energy and Climate Economics. Center for Economic Studies & Ifo Institute. 39 pp.

Levitus, S., J.I. Antonov, T.P. Boyer, O.K. Baranova, H.E. Garcia, R.A. Locarnini, A.V. Mishonov, J.R. Reagan, D. Seidov, E.S. Yarosh and M.M. Zweng, 2012. World Ocean Heat Content and Thermosteric Sea Level Change (0–2000m) 1955–2010, *Geophysical Research Letters* 39: L10603.

Lewis, N., 2018. Abnormal climate response of the DICE IAM – a trillion dollar error? April 22. At https://www.nicholaslewis.org/tag/climate-sensitivity/ [accessed October 28, 2020].

Lewis, N. and J.A. Curry, 2018. The Impact of Recent Forcing and Ocean Heat Uptake Data on Estimates of Climate Sensitivity, *Journal of Climate* 31(August): 6051-6071. doi: 10.1175/JCLI-D-17-0667.1

Lewis, N. and J.A. Curry, 2015. The Implications for Climate Sensitivity of AR5 Forcing and Heat Uptake Estimates, *Climate Dynamics* 45: 1009-1023.

Lindzen, R.S., 2020. An Oversimplified Picture of the Climate Behavior Based on a Single Process can lead to Distorted Conclusions, *European Physical Journal Plus* 135:162. doi: 10.1140/epjp/s13360-020-00471-z.

Lomborg, B., 2007. *Cool It. The Skeptical Environmentalist's Guide to Global Warming*. New York: Alfred A. Knopf.

Maher, N., F. Lehner and J. Marotzke, 2020. Quantifying the Role of Internal Variability in the Temperature we Expect to Observe in the Coming Decades, *Environmental Research Letters* 15(5): 054014. Doi: 10.1088/1748-9326/ab7d02.

McGuffie, K. and A. Henderson-Sellers, 2009. *A Climate Modeling Primer* 3rd ed. Chichester, UK: John Wiley & Sons.

McIntyre, S. and R. McKitrick, 2009. Proxy Inconsistency and Other Problems in Millennial Paleoclimate Reconstructions, *Proceedings of the National Academy of Sciences* 106(6):E10, February 2. https://doi.org/10.1073/pnas.0812509106.

McKitrick, R., 2015. The Hockey Stick: A Retrospective. Chapter 14 in *Climate Change: The Facts* edited by Alan Moran. Woodsville, NH: Stockade Books. 2014.

McKitrick, R. and J. Christy, 2020. Pervasive Warming Bias in CMIP6 Tropospheric Layers, *Earth and Space Science* 7: e2020EA001281. https://doi.org/10.1029/2020EA001281.

McKitrick, R. and J. Christy, 2019a. A Test of the Tropical 200- to 300-hPa Warming Rate in Climate Models, *Earth and Space Science* 5(9): 529-536. doi: 10.1029/2018EA000401.

McKitrick, R. and J. Christy, 2019b. Assessing Changes in US Regional Precipitation on Multiple Time Scales, *Journal of Hydrology* 578: 124074, ISSN 0022-1694, doi: 10.1016/j.jhydrol.2019.124074.

McKitrick, R.R. and P.J. Michaels, 2007. Quantifying the Influence of Anthropogenic Surface Processes and Inhomogeneities on Gridded Global Climate Data, *Journal of Geophysical Research*, 112, D24S09, doi:10.1029/2007JD008465.

McKitrick, R.R. and P.J. Michaels, 2004. A Test of Corrections for Extraneous Signals in Gridded Surface Temperature Data, *Climate Research* 26: 159-173.

McKitrick, R.R. and N. Nierenberg, 2011. Socioeconomic Signals in Climate Data, *Journal of Economic and Social Measurement* 35(3,4): 149-175.

McKitrick, R. R. and T. Vogelsang, 2014. HAC-Robust Trend Comparisons among Climate Series with Possible Level Shifts, *Environmetrics 25*(7): 528-547.

Millar, R.J., J.S. Fuglestvedt, P. Friedlingstein, J. Rogelj, M.J. Grubb, H.D. Matthews, R.B Skeie, P.M. Forster, D.J. Frame and M.R. Allen, 2017. Emission Budgets and Pathways Consistent with Limiting Warming to 1.5°C, *Nature Geoscience* 10: 741-747. doi: 10.1038/ngeo3031.

Monckton, C., 2019. CMIP6 Models Overshoot: Charney Sensitivity is not 4.1 K but < 1.4 K. October 6. At https://wattsupwiththat.com/2019/10/08/cmip6-models-overshoot-charney-sensitivity-is-not-4-1-k-but-1-4-k/ [accessed May 4, 2020].

Moore, P., 2016. The Positive Impact of Human CO2 Emissions on the Survival of Life on Earth. June. 24pp. Frontier Center for Public Policy. At https://fcpp.org/wp-content/uploads/2016/06/Moore-Positive-Impact-of-Human-CO2-Emissions.pdf [accessed May 7, 2021].

NOAA, 2018. WOA 2018 Data Access: Statistical Mean of Temperature on 1° Grid for All Decades. https://www.nodc.noaa.gov/cgi-bin/OC5/woa18/woa18.pl [accessed April 16, 2020].

Nordhaus, W.D., 2019. Climate Change: The Ultimate Challenge for Economics, *American Economic Review* 109(6): 1991-2014. doi: 10.1257/aer.109.6.1991

Nordhaus, W.D., 2018a. Evolution of Assessments of the Economics of Global Warming: Changes in the DICE Model, 1992-2017, *Climatic Change* 148(4): 623-640.

Nordhaus, W.D., 2018b. Projections and Uncertainties about Climate Change in an Era of Minimal Climate Policies, *American Economic Journal: Economic Policy* 10(3): 333-360.

Nordhaus, W.D., 2017. Revisiting the Social Cost of Carbon, *PNAS* 114(7): 1518-1523.

Nordhaus, W.D., 2013. Integrated Economic and Climate Modeling. Chapter 16 in *Handbook of Computable General Equilibrium Modeling, Volume 1A, 1st Edition* (pp.1069-1131) edited by P. Dixon and D. Jorgenson. Dordrecht, NL: Elsevier. (DICE model found at https://sites.google.com/site/williamdnordhaus/dice-rice [accessed 25 February 2019])

Norstad, J., 2011. An Introduction to Utility Theory. Evanston, IL: Northwestern University. 26 pp.

Otto, A., F.E.L. Otto, O. Boucher, J. Church, G. Hegerl, P. Forster, N.P. Gillett, J. Gregory, G. Johnson, R. Knutti, N. Lewis, U. Lohmann, J. Marotzke, G. Myhre, D. Shindell, B. Stevens and M.R. Allen, 2013. Energy Budget Constraints on Climate Response, *Nature Geoscience* 6: 415-416. doi: 10.1038/ngeo1836.

Pielke, Jr, R., 2018. *The Rightful Place of Science: Disasters and Climate Change*. 2nd edition. Tempe, AZ: Consortium for Science, Policy and Outcomes.

Pierrehumbert, R.T., 2011. *Principles of Planetary Climate*. Cambridge, UK: Cambridge University Press.

Pindyck, R.S., 2017. The Use and Misuse of Models for Climate Policy, *Review of Environmental Economics and Policy* 11(1): 100-114. doi:10.1093/reep/rew012.

Pindyck, R.S., 2013. Climate Change Policy. What do the Models Tell Us? *Journal of Economic Literature* 51(3): 860-872.

Phillips, P.C.B., T. Leirvik and T. Storelvmo, 2020. Econometric Estimates of Earth's Transient Climate Sensitivity, *Journal of Econometrics* 214(1): 6-32.

Pretis, F., 2020. Econometric Modelling of Climate Systems: The Equivalence of Energy Balance Models and Cointegrated Vector Autoregressions, *Journal of Econometrics* 214(1): 256-273.

Reidmiller, D.R., C.W. Avery, D.R. Easterling, K.E. Kunkel, K.L.M. Lewis, T.K. Maycock and B.C. Stewart, 2017. *U.S. Global Change Research Program: Fourth National Climate Assessment. Volume II: Impacts, Risks, and Adaptation in the United States, Summary*. Washington, DC. Retrieved from: https://nca2018.globalchange.gov/ [accessed May 6, 2021].

Rezai, A. and F. van der Ploeg, 2016. Intergenerational Inequality Aversion, Growth, and the Role of Damages: Occam's Rule for the Global Carbon Tax, *Journal of the Association of Environmental and Resource Economists* 3(2): 493-522.

Riahi, K., D.P. van Vuuren, and 43 others, 2017. The Shared Socioeconomic Pathways and their energy, land use, and greenhouse gas emissions implications: An overview, *Global Environmental Change* 42: 153-168.

Richard, K., 2019. Scientists: The Entirety of The 1979-2017 Global Temperature Change Can Be Explained by Natural Forcing, October 28. https://notrickszone.com/2019/10/28/scientists-the-entirety-of-the-1979-2017-global-temperature-change-can-be-explained-by-natural-forcing/ [accessed May 7, 2021].

Richardson, M., K. Cowtan, E. Hawkins and M.B. Stolpe, 2016. Reconciled Climate Response Estimates from Climate Models and the Energy Budget of Earth, *Nature Climate Change* 6: 931-935. doi: 10.1038/nclimate3066.

Rutledge, D., 2014. Coal and the IPCC. Climate Etc. Blog, April 22 April. At: https://judithcurry.com/2014/04/22/coal-and-the-ipcc/ [accessed May 7, 2021].

Schildknecht, D., 2020. Saturation of the Infrared Absorption by Carbon Dioxide in the Atmosphere, *International Journal of Modern Physics B* 34(30): 2050293. https://doi.org/10.1142/S0217979220502938.

Smirnov, B.M., 2020. *Global Atmospheric Phenomena Involving Water. Water Circulation, Atmospheric Electricity, and the Greenhouse Effect*. Cham, Switzerland: Springer Nature.

Spencer, R. W., and W. D. Braswell, 2010. On the Diagnosis of Radiative Feedback in the Presence of Unknown Radiative Forcing, *Journal of Geophysical Research* 115: doi:10.1029/2009JD013371.

Svensmark, H., M.B. Enghoff, N. Shaviv and J. Svensmark, 2017. Increased Ionization Supports Growth of Aerosols into Cloud Condensation Nuclei, *Nature Communications* 8: Article 2199. doi: 10.1038/s41467-017-02082-2.

Tol, R.S.J., 2014. *Climate Economics. Economic Analysis of Climate, Climate Change and Climate Policy*. Cheltenham, UK: Edward Elgar. (FUND model found at: http://www.fund-model.org/source-code)

Trenberth, K.E. and L. Smith, 2005. The Mass of the Atmosphere: A Constraint on Global Analyses, *Journal of Climate* 18(6): 864-875.

Trenberth, K.E. and C.J. Guillemot, 1994. The Total Mass of the Atmosphere, *Journal of Geophysical Research* 99(D11): 23,079-23,088.

United Nations (2015, December). *Paris Climate Agreement.* At: https://unfccc.int/process-and-meetings/the-paris-agreement/the-paris-agreement [accessed May 6, 2021].

van Kooten, G.C., 2021. *Applied Welfare Economics, Trade and Agricultural Policy Analysis*. Toronto, ON: University of Toronto Press.

van Kooten, G.C., 2020. How effective are Forests in Mitigating Climate Change? *Forest Policy & Economics* 120(November): 102295. https://doi.org/10.1016/j.forpol.2020.102295.

van Kooten, G.C., 2013. *Climate Change, Climate Science and Economics: Prospects for a Renewable Energy Future*. Dordrecht, NL: Springer. (466pp.)

van Kooten, G.C. and C.M.T. Johnston, 2016. The Economics of Forest Carbon Offsets, *Annual Review of Resource Economics* 8(1): 227-246.

van Kooten, G.C., P. Withey and C.M.T. Johnston, 2021. Climate Urgency and the Timing of Carbon Fluxes. Draft 14pp. Under review at *Biomass and Bioenergy*.

van Vuuren, D.P., J. Edmonds, M. Kainuma, K. Riahi, A. Thomson, K. Hibbard, G.C. Hurtt, T. Kram, V. Krey, J.-F. Lamarque, T. Masui, M. Meinshausen, N. Nakicenovic, S.J. Smith and S.K. Rose, 2011. The Representative Concentration Pathways: An Overview, *Climatic Change* 109(5): 1573-1480.

van Wijngaarden, W.A. and W. Happer, 2020. Dependence of Earth's Thermal Radiation on Five Most Abundant Greenhouse Gases, *Atmospheric and Oceanic Physics* arXiv: 2006.03098.

van Wijngaarden, W.A. and W. Happer, 2019. Methane and Climate. 24pp. Arlington, VA: CO2 Coalition. At https://wvanwijngaarden.info.yorku.ca/publications/ [accessed May 6, 2021].

Voosen, P., 2016. Climate Scientists Open Up their Black Boxes to Scrutiny, *Science* 354(6311): 401-402. DOI: 10.1126/science.354.6311.401.

Wallace, J.M. and P.V. Hobbs, 2006. *Atmospheric Science. An Introductory Survey. Second Edition*. Amsterdam, NL: Elsevier.

Zelinka M.D., T.A. Myers, D.T. McCoy, S. Po-Chedley, P.M. Caldwell, P. Ceppi, S.A. Klein and K.E. Taylor, 2020. Causes of Higher Climate Sensitivity in CMIP6 Models, *Geophysical Research Letters* 47(1): e2019GL085782. https://doi.org/10.1029%2F2019GL085782.

Zharkova, V.V., S.J. Shepherd, S.I. Zharkov and E. Popova, 2019. Oscillations of the Baseline of Solar Magnetic Field and Solar Irradiance on a Millennial Timescale, *Scientific Reports* 9(1): 2045-2322. doi: 10.1038/s41598-019-45584-3.

Zhu, J., C.J. Poulsen and B.L. Otto-Bliesner, 2020. High Climate Sensitivity in CMIP6 Model not Supported by Paleoclimate, *Nature Climate Change* April 30. doi: 10.1038/s41558-020-0764-6.

APPENDIX

Table A.1: Climate Feedback and Scaling Factors Based on Observational Data

	Historic temperatures		All proxies		Proxies without tree rings	
Parameter	Median	66.6% CI	Median	66.6% CI	Median	66.6% CI
λ	1.03	[0.90 1.49]	1.19	[0.67 3.68]	1.47	[0.74 4.22]
a_{anth}	0.99	[0.76 1.17]	0.68	[0.55 1.08]	0.10	[-0.75 0.36]
a_{volc}	0.34	[0.20 0.53]	0.53	[0.27 1.27]	0.26	[0.08 0.84]
a_{Lsol}	1.28	[-2.14 5.99]	6.07	[3.16 16.50]	14.90	[7.38 42.22]
a_{Hsol}	0.42	[-0.58 1.38]	0.58	[-1.60 2.54]	-0.68	[-3.05 0.27]

Source: de Larminat (2019, Table 2)